CHAPTER IV

RESULTS AND DISCUSSION

4.1 Preparation of Polyisoprene Latexes

The preparation and characterization of polymer latex have a long history. Traditionally, latex (polymer) preparation needs four essential elements: monomer, initiator, surfactant, and dispersion media. All these parameters, together with preparation conditions, affect latex characteristics.

Synthetic polymeric colloids or latexes are usually synthesized by emulsion polymerization of vinyl monomers. Emulsion polymerization is a heterogeneous reaction process in which hydrophobic monomers are dispersed in a continuous aqueous phase with the aid of an emulsifier system and polymerized with free-radical initiators. The product, a colloidal dispersion of the polymer, is called a latex.

Polyisoprene latexes were prepared by free-radical conventional emulsion polymerization in the 500-cm^3 bottle polymerizer. As mentioned previously in Chapter 3 that a systematic study has been organized to elucidate the effect of variable parameters (surfactant, monomer, initiator concentration and reaction temperature) on the polyisoprene latex characteristics emphasizing on the latex size. For this purpose, technological practices rather than theoretical aspects are considered.

4.1.1 Effect of Surfactant Concentration on Particle Size

Sodium dodecyl sulfate was used as a surfactant. Under the constant conditions (temperature 60°C, initiator concentration 8.02×10^{-3} mol dm^{-3} and monomer concentration 2.82 mol dm^{-3}), the effect of surfactant concentration on the particle size was examined. The results are shown in Table 4-1. The same trend of decreasing particle size with increasing surfactant concentration has been observed in the other emulsion polymerization system by other researchers (112-115).

Table 4-1 Dependence of the polymer particle diameter on the surfactant concentration

Run	SDS	Gravimetric analysis		Particle size
	(mol dm^{-3})	%solid content	%conversion	(nm)
S00	-	1.9	9.0	237
S01	7.43×10^{-3}	17.3	80.7	116
S02	1.48×10^{-2}	18.1	83.6	94
S03	3.64×10^{-2}	19.6	88.4	68
S04	7.08×10^{-2}	20.6	96.7	59

Polymerizations were carried out at 2.82 mol dm^{-3} isoprene monomer; 8.02×10^{-3} mol dm^{-3} $Na_2S_2O_8$; 6.88×10^{-2} mol dm^{-3} $NaHCO_3$; 9.34×10^{-3} mol dm^{-3} *n*-DM at 60°C.

It is well known that the emulsifier concentration has a strong effect on the average particle diameter, and number of polymer particles (N_t) formed in the emulsion polymerization. According to the Smith-Ewart (54) micellar theory, the relationship between these parameters can be expressed mathematically as

$$N_t \approx [\text{emulsifier}]^{0.6} \qquad (4\text{-}1)$$

This equation has been proved to be valid occasionally for emulsion polymerization of water-insoluble monomers such as styrene using an anionic surfactant (25). By increasing emulsifier concentration, the number of polymer particles (N_t) increases (115) and the average particle diameter decreases. Increasing emulsifier concentration accelerates the rate of polymerization because of the increasing number of latex particles. This reduces the particle size at the expense of the number of particles. Many mathematical models for the prediction of particle growth in emulsion polymerization have been developed, from which Lopez de Arbina et al. (116) is one of preferably used kinetics.

4.1.2 Effect of Monomer Concentratioon Particle Size

The effect of the amount of the monomer on the particle size was examined at a constant temperature and other variables, which details are listed in Table 4-2. By increasing the amount of monomer for polymerization, the particle size increased because the bigger-sized nuclei produced large-sized particles. In addition, the longer time for the latex particles to coalescence also produced the larger particles.

Table 4-2 Dependence of the polymer particle diameter on the monomer concentration

Run	Monomer Concentration (mol dm^{-3})	Particle size (nm)
M01	2.82	59
M02	3.37	63
M03	3.86	67

Polymerizations were carried out at 8.02 × 10^{-3} mol dm^{-3} $Na_2S_2O_8$; 7.08 × 10^{-2} mol dm^{-3} SDS; 6.88 × 10^{-2} mol dm^{-3} $NaHCO_3$; 9.34 × 10^{-3} mol dm^{-3} *n*-DM at 60°C.

4.1.3 Effect of the Initiator Concentration on Particle Size

The result for the variation of the particle diameter as a function of the initial concentration of initiator at 60°C, constant concentration of the monomer and surfactant are given in Table 4-3. The result clearly shows that a decrease in the initiator concentration, under constant conditions (monomer concentration 2.82 mol dm^{-3}, surfactant concentration 7.08 × 10^{-2} mol dm^{-3}), increased the polymer particle size. The same observation of decreasing particle size with increasing initiator concentration has been reported, hundred of papers are derived from the Hunkins/Smith-Ewart assumptions (26, 113).

Sodium persulfate dissociates into two sulfate radical anions which can initiate the polymerization (26). These radicals may propagate in the aqueous phase to form oligoradicals by adding monomer molecules dissolved in the aqueous phase. Particle nucleation begins at this point via one mechanism or another, forming polymer particles, from monomer droplets. These monomer swollen polymer particles become the main sites for further propagation reactions to promote particle growth. This is responsible for the ability to simultaneously increase the polymerization rate. By increasing polymerization rate, the number of particle increases and their size decreases.

Table 4-3 Dependence of the polymer particle diameter on the initiator concentration

Run	Initiator Concentration ($mol\ dm^{-3}$)	Particle size (nm)
I01	8.03×10^{-4}	217
I02	4.01×10^{-3}	111
I03	8.02×10^{-3}	59

Polymerizations were carried out at 2.82 $mol\ dm^{-3}$ isoprene monomer; 7.08×10^{-2} $mol\ dm^{-3}$ SDS; 6.88×10^{-2} $mol\ dm^{-3}$ $NaHCO_3$; 9.34×10^{-3} $mol\ dm^{-3}$ *n*-DM at 60°C.

4.1.4 Effect of Temperature on Particle Size

The emulsion polymerization of isoprene monomer was carried at two different temperatures, 60 and 70°C. The effect of temperature on the final particle size was investigated. The other factors such as initiator, monomer, surfactant and ionic strength were held constant. The results are shown in Table 4-4.

Table 4-4 Dependence of the polymer particle diameter on the reaction temperature

Run	Reaction temperature (°C)	Particle size (nm)
T60	60	59
T70	70	53

Polymerizations were carried out at 2.82 mol dm^{-3} isoprene monomer; 8.02 × 10^{-3} mol dm^{-3} $Na_2S_2O_8$; 7.08 × 10^{-2} mol dm^{-3} SDS; 6.88 × 10^{-2} mol dm^{-3} $NaHCO_3$; 9.34 × 10^{-3} mol dm^{-3} *n*-DM.

It is not convenient to carry out the polymerization at temperatures below 60°C because of the slow rate of initiator decomposition. Table 4-4 shows that the diameter decreases when the reaction temperature increased as the temperature must be high enough to give a reasonable rate of initiator decomposition. High temperature provides a large number of radicals, and therefore a large number of nuclei are also generated. Solubility is increased by increasing temperature. This means that more monomer dissolves in the solvent, which leads to an increase in the number of polymer nuclei in a sequential even of polymerization. More nuclei produce more particles; hence the particle size is decreased. However, temperature is a useful parameter, which normally controls particle size. However, the low boiling point monomers such as isoprene and butadiene can evaporate rapidly at high temperatures and a low solid content could result. Polymerization reactions in a laboratory scale were not therefore carried out at the temperature above 70°C, evertheless, they can be carried out under pressure at higher temperatures and frequently are in industry.

4.2 Grafting

4.2.1 Mechanism of Grafting

4.2.1.1 The Initiation Process

Hydroperoxide initiators (in the form of RO-OH) such as cumene hydroperoxide, CHP are known to dissociate in the presence of an oxidizable metal ion to yield a peroxyl radical (117) (Figure 4-1) and a hydroxide ion. It is not known if the presence of this metal ion is still required to form the peroxyl radical when the peroxide is the inherent species of some co-initiator added such as TEPA, which will enable the formation of a redox couple. The exact nature of the radicals formed by TEPA in its reaction with alkyl RO-OH is unknown. A possible route whereby the RO-OH species undergoes a reduction reaction to form the alkyloxyl radical and an OH^- ion is shown below (eq 4-2). The oxidizable metal ion has been replaced by a TEPA molecule, which has been shown to be oxidized to a positively charged radical. This method has been selected to balance charges and electrons but as previously mentioned it is not known what happens to the TEPA and what role metal ions play.

(a) (b)

Figure 4-1 Structures of the (a) cumyloxyl radical and (b) *t*-butyloxyl radical.

$$\text{RO-OH} + \text{TEPA} \longrightarrow \text{RO}^{\bullet} + \text{OH}^{-} + \text{TEPA}^{+\bullet} \qquad (4\text{-}2)$$

where RO-OH = alkyl hydroperoxide (CHP),

TEPA = tetraethylene pentamine (TEPA),

$\text{RO}^{\bullet}$ = alkyloxyl radical,

$\text{TEPA}^{+\bullet}$ = amine cationic radical.

The initiating radical ($\text{RO}^{\bullet}$) now has several possible fates. It can react with polymer by an addition to the double bonds (eq 4-3), or an abstraction of a proton (eq 4-4) or it may react with a non-polymeric species by recombination with a second like radical (eq 4-5) or addition to a monomer (eq 4-6).

$$\text{RO}^{\bullet} + \text{NR} \longrightarrow \text{RO–NR}^{\bullet} \qquad (4\text{-}3)$$

$$\text{RO}^{\bullet} + \text{NR-H} \longrightarrow \text{RO–H} + \text{NR}^{\bullet} \qquad (4\text{-}4)$$

$$\text{RO}^{\bullet} + \text{RO}^{\bullet} \longrightarrow \text{RO–OR} \qquad (4\text{-}5)$$

$$\text{RO}^{\bullet} + \text{M} \longrightarrow \text{RO–M}^{\bullet} \qquad (4\text{-}6)$$

where $\text{NR}^{\bullet}$ = natural rubber backbone radical,

M = monomer

Use of relatively bulky oxygen-centred radicals, such as the cumyloxyl radical, will favor absorption over addition (27, 118) In addition, more nucleophilic radicals such as cumyloxyl radicals have been seen to favor the hydrogen absorption reaction over addition to double bonds.

Based upon this set of reaction mechanisms, we see that the reaction of alkyloxyl radicals with monomer may provide a means by which ungrafted polymer can be formed to compete with the grafting process.

4.2.1.2 Polymerization and Termination

The next set of reaction steps comprises the reaction of the polymer graft site, created by the abstraction of a proton by the cumyloxyl radical, to commence the polymerization of monomer. The polymeric radical may react with the monomer via addition (eq 4-7) or transfer to monomer (eq 4-8) to form grafted and free polymers, respectively, or it may recombine with another polymeric radical species (eq 4-9). There is also a possibility of termination with an initiator radical (eq 4-10).

$$NR^{\bullet} + M \longrightarrow NR{-}M^{\bullet} = R_1^{\bullet} \qquad (4\text{-}7)$$

$$NR^{\bullet} + M \longrightarrow NR + M^{\bullet} \qquad (4\text{-}8)$$

$$NR^{\bullet} + NR^{\bullet} \longrightarrow NR{-}NR \qquad (4\text{-}9)$$

$$NR^{\bullet} + RO^{\bullet} \longrightarrow NR{-}OR \qquad (4\text{-}10)$$

where $M^{\bullet}$ = monomeric radical,

$R_1^{\bullet}$ = growing polymer chain with one monomeric unit grafted.

The new growing grafted polymer chain ($R_i^\bullet$) can undergo several reactions (which are also applicable to the $NR^\bullet$ species.) It may continue to grow by addition of the monomer (4-11), termination with the monomeric radical (or other small radical species,) (4-12) or another growing chain (4-13). The growing polymer chain may also transfer to the monomer (4-14).

$$R_i^\bullet + M \longrightarrow R_{i+1}^\bullet \tag{4-11}$$

$$R_i^\bullet + M^\bullet \longrightarrow R_{i+1} \tag{4-12}$$

$$R_i^\bullet + R_j^\bullet \longrightarrow R_{i+j} \tag{4-13}$$

$$R_i^\bullet + M \longrightarrow R_i + M^\bullet \tag{4-14}$$

where R_x , $R_x^\bullet$ = polymer chains and growing polymer chains of length x.

4.2.2 'Hairy Layer' Generated by the Grafting Reaction

The properties of the modified latexes are summarized in Table 4-5. While the unmodified polyisoprene latex is colloidally unstable at low pH, grafted latexes prepared by the second-stage polymerization were stable for a period of up to one week even at pH 2. The effect of changing pH from 12 to 2 on the apparent particle size (hydrodynamic diameter) of the modified latexes, as measured by dynamic light scattering (DLS), is presented in Figure 4-2. No attempt was made to remove any poly(DMAEMA) homopolymer generated in the aqueous phase before these measurements were carried out, since this is unnecessary because of the small size of the homopolymer molecules relative to the latex particles (dynamic light scattering is most sensitive to large scattering entities). The fluctuation of the refractive index of the aqueous phase due to dissolved polymer is negligible because it is necessary to convert the DLS signals into particle size. The differences in refractive index between the core polyisoprene and poly(DMAEMA) shell (hairy layer) present difficulties in determining particle size accurately. Even though the sizes determined are semi-quantitative, the observed trends are sufficiently accurate for the purposes of this study and representative of the phenomena being observed.

Table 4-5 Properties of latexes formed by the polymerization of DMAEMA in the presence of small seed

Parameter	TEPA feed time (h)				
	0.5	1	2	4	6
Conversion (%)	98.4	97.6	98.5	97.9	98.1
Solid content (%)	14.4	14.3	14.4	14.3	14.3
Gel fraction (%)	64.3	65.1	62.4	61.4	54.5
Particle diameter (nm) at *p*H = 9	113	106	95	84	72
Ungrafted polyisoprene (%)	18.7	14.6	14.6	16.9	20.6
Ungrafted poly(DMAEMA) (%)	19.1	18.4	17.4	16.8	15.3
GE %	50.9	52.6	55.2	56.8	60.5

The pH was changed by addition of HCl or NaOH. The acidic or basic addition changes the ionic strength and the corresponding effects due to changes in ionic strength. The pH changes in our system caused by the addition of HCl are not higher than 10 mM introduce a relatively small effect on both colloidal stability and chain conformation of the polyelectrolyte (see, e.g. (118) for the magnitude of changes in these properties brought about by changes in ionic strength).

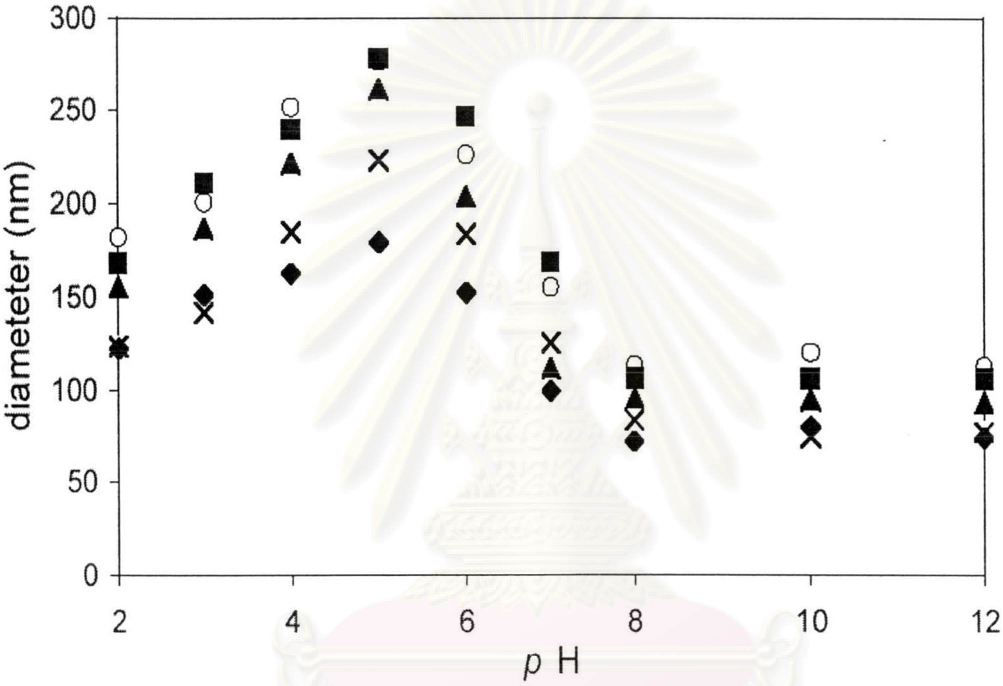

Figure 4-2 Particle size by DLS of the modified latex prepared at different TEPA feed times at 15 °C as a function of *p*H: (○) 0.5h, (■) 1h, (▲) 2h, (×) 4h, and (◆) 6h TEPA feed time. The seed had an unswollen diameter of 59 nm.

It was found that the particle sizes (hydrodynamic diameter) of modified latexes were nearly constant at high pHs (from pH 12 to 8), then increased to reach a maximum value at pH 5 and decreased with further decreases in pH. These results are consistent with extensive grafting of a poly(DMAEMA) hairy layer on the polyisoprene particles. The trend in apparent particle diameter observed could be explained by protonation of the nitrogen on the poly(DMAEMA) chains grafted onto the particle surface, leading to chain expansion. At pH < 5 the size decreases because increasing the ionic strength decreases the effective repulsion between the charged poly(DMAEMA) chains causing them to be less expanded from the surface of the particles. Similar trends have been observed by Prescott et al. (120) for other polyelectrolytes.

As the feed rate is increased, the diameter of the uncharged particles and the grafting efficiency increases while the gel fraction remains relatively constant. The apparent decrease in thickness of the hairy layer decreases as the length of the feed period is extended, i.e., the radical flux was reduced. This is counterintuitive, as we could expect that a reduced radical flux at similar monomer concentrations would lead to a longer kinetic chain length in polymer and therefore a thicker hydrophilic layer was found ultimately in conventional free-radical polymerization. One possibility is that at a higher radical flux there are more polymerization reactions within the particles, in contrary to the assumptions of the topology-controlled mechanism. This would lead to an increase in particle diameter unconnected with the hairy layer; however, this would be expected to result in a maximum increase in particle radius of no more than approximately 20%. Another possibility is that the higher radical flux gives a more extensive layer by generating a larger number of grafted chains on the surface. As such, this is a plausible explanation for the observations.

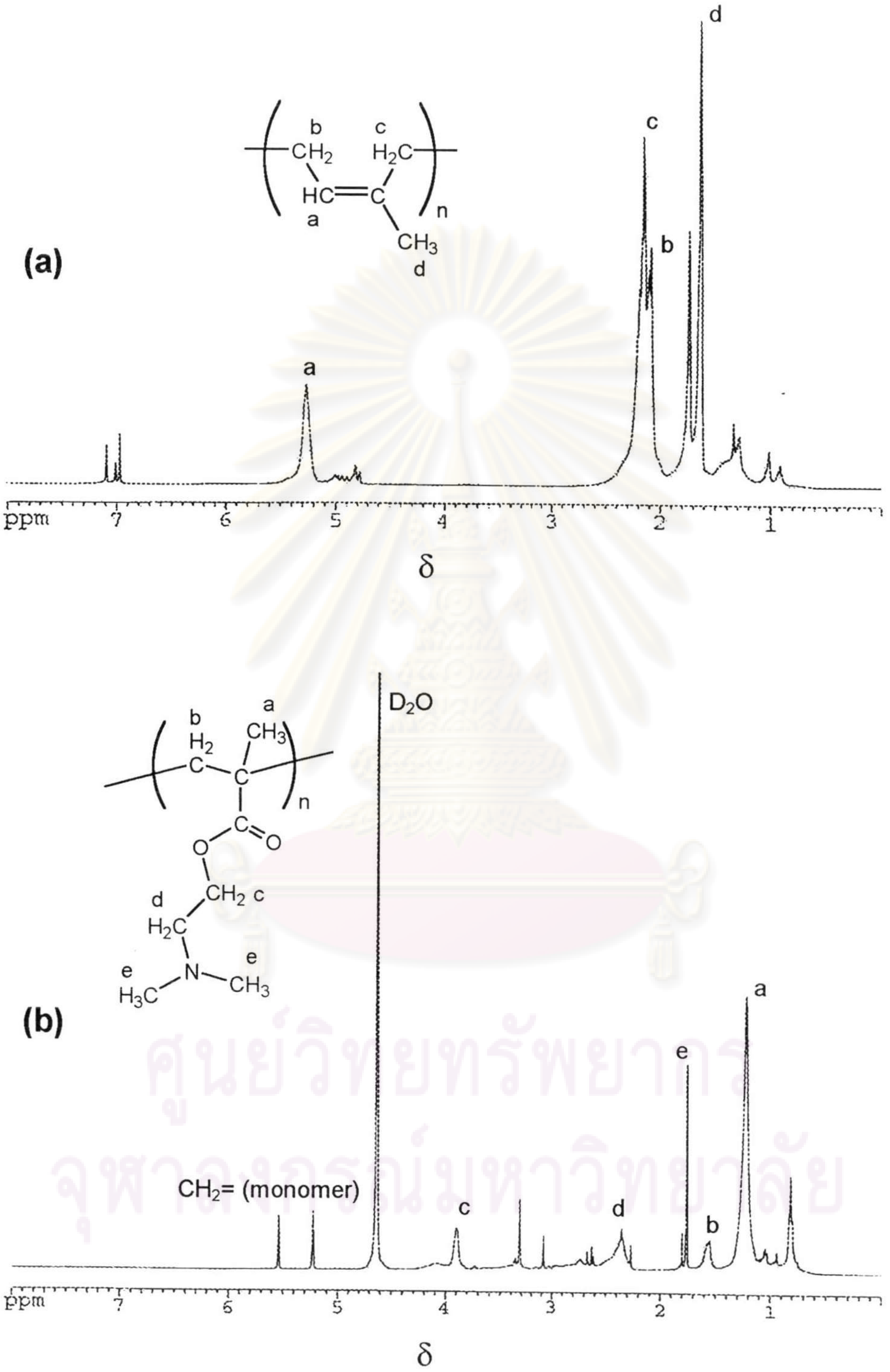

Figure 4-3 ^{1}H-NMR spectra of (a) organic extraction product of the modified polyisprene, and (b) aqueous extraction product of the modified polyisoprene at 1 h TEPA-feed time.

NMR spectra recorded for the organic extraction product of the modified polyisoprene latex, shown in Figure 4-3(a), did not show any characteristic peaks of poly(DMAEMA), but did show the presence of polyisoprene. Conversely, the NMR spectra recorded for the aqueous extraction product of the modified polyisoprene latex (Figure 4-3(b)) did not show any characteristic peaks of polyisoprene, but did show the presence of poly(DMAEMA). This implies that all grafted material remained in the insoluble fraction.

4.2.3 Kinetic of Grafting Reaction from Microcalorimetry

From the experiment, the RC1 reaction calorimeter provides values of heat of reaction as a function of time, determined once every 20 s. the typical data are shown in Figure 4-4.

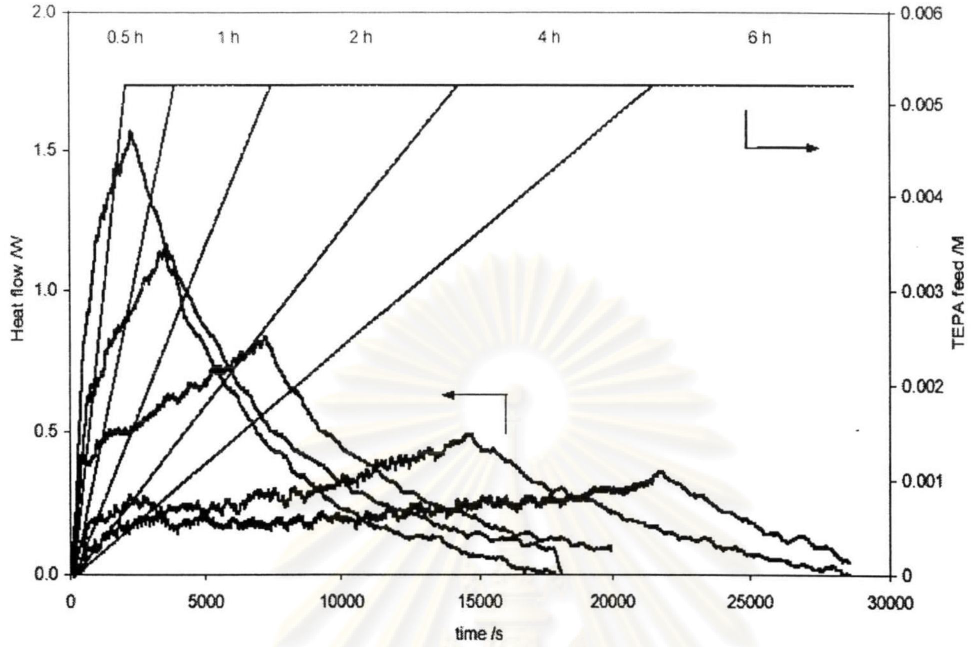

Figure 4-4 Grafting of DMAEMA onto a polyisoprene latex: heat of reaction against time curves at different TEPA feed rates. In all cases the final TEPA concentration was 5.3×10^{-3} M.

Calorimetric data were processed to obtain the monomer concentration as a function of time using eq 3-2; as stated, these results should be semi-quantitative. The data so obtained are given in Figure 4-5 as a plot of ln[M] as a function of time. This plot would be linear if classical free radical solution kinetics were obeyed. The reaction rates obtained using eq 3-1 and the initiator feed profile are given in Figure 4-6 for comparing the large and small latex at the same initiator feed profile, and in Figure 4-4 for the small latex for different initiator feed profiles, given as heat evolution, which is proportional to rate.

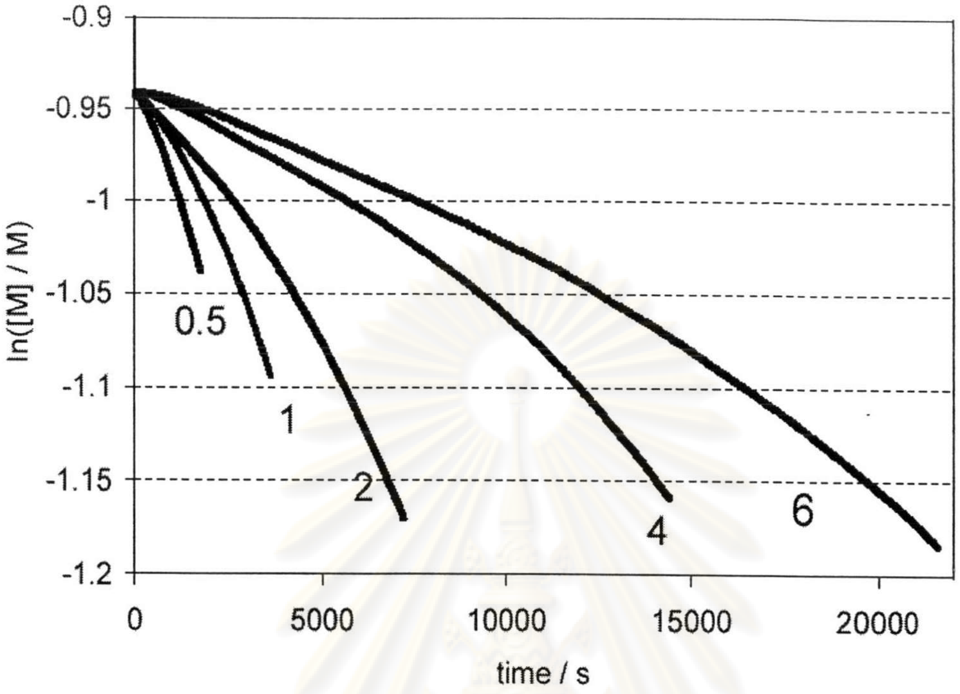

Figure 4-5 Variation of DMAEMA concentration with time during polymerizations at different TEPA feed times: 0.5, 1, 2, 4 and 6 h, as indicated. To isolate the chain-growth events in the presence of constant monomer feed, each data set is truncated at the time of cessation of TEPA feed.

There are three possible loci of polymerization in this system: grafting reactions which would lead to polymerization of chains attached to the particles (i.e., the topology-controlled mechanism); homogeneous polymerization in the water phase (i.e. producing the ungrafted DMAEMA homopolymer); and polymerization within the interior of the latex particles. The concentration of monomer would be different in each of these three loci. One then has:

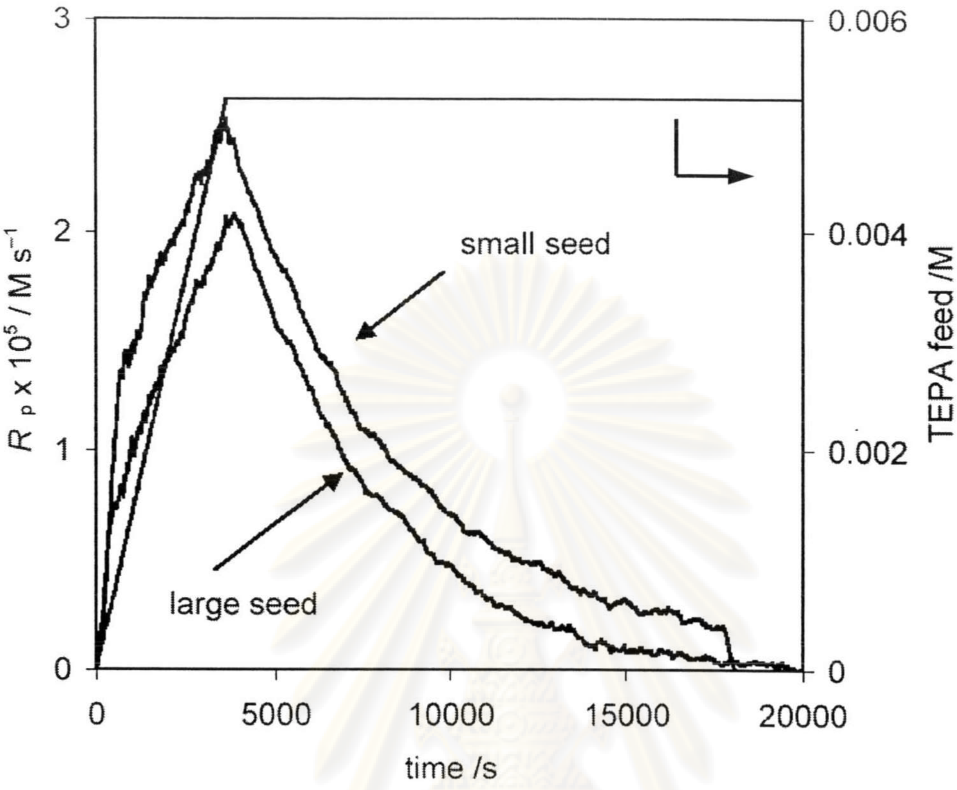

Figure 4-6 Rates of polymerization as a function of time for different polyisoprene seed sizes, 59 and 137 nm (conditions of Table 3-3); TEPA feed rates are shown as a smooth line.

$$R_p = k_p \left([\mathrm{M}]_w [\mathrm{R}^\bullet]_w + [\mathrm{M}]_{hl} [\mathrm{R}^\bullet]_{hl} + [\mathrm{M}]_p [\mathrm{R}^\bullet]_p \right) \qquad (4\text{-}15)$$

where $[\mathrm{R}^\bullet]$ is the radical concentration and the subscripts (w, hl, and p) refer to the water, hairy-layer and particle phases. Polymerization in the interior of the particle is possible because there are small but significant amounts of both DMAEMA and TEPA inside the particles at the pH used here. Accurate quantification of the polymerization kinetics, and an area for future study, requires measurement of the partitioning of these species between the aqueous and polyisoprene phases.

The data of Figure 4-6 compare the rates of two polymerizations (Table 3-4) with the same TEPA feed profile, but in which the particle sizes differ by a factor of ~2, the number of density for latex particles in the reactor, N_p, differs by a factor of 10, the total surface area of particles differs by a factor of 2 and the total mass of seed (and hence the particle volume) is the same. The data of Figure 4-6 show that there is only a slight dependence (~25%) of the rate on the seed-particle size. We now consider various explanations for this observation, which gives the large differences in particle number and surface area.

a) If the only locus of polymerization were the water phase (unassociated with the particles), then R_p would be independent of both total surface area and of N_p.

b) If the only locus of polymerization were the interior of the particles, and initiation efficiency were 100%, and the intra-particle kinetics were "pseudo-bulk" (i.e., kinetically the same as in a bulk or solution polymerization (25)), then again R_p would be independent of both total surface area and of N_p. If initiator efficiency were significant less than 100%, and/or pseudo-bulk kinetics were not obeyed, then this independence would not hold.

c) If the locus of polymerization were exclusively from polymer chains initiated at, and tethered to, the particle surface (topology-controlled polymerization), one would expect a strong dependence of the rate on total surface area.

Now, the colloidal stability data show unambiguously that there is a significant amount of poly(DMAEMA) grafted to the particle surface. However, this polymerization locus cannot be the dominant one, for the reasons given in c) above. It is unlikely for b) to be the dominant event, because the hydrophilicity of TEPA and hydrophobicity of CHP suggest that significant radical generation must occur at the interface, and this is likely to be relatively inefficient. For these reasons, it is likely that the dominant locus of polymerization is within the water phase, initiated by radicals formed at the interface or within the particles which do not abstract but instead go into the water phase, and/or from DMAEMA monomeric radicals, which arise from transfer to water-phase monomer from a polymerizing chain whose radical end is in the water phase but which is tethered to the particle.

Although the data of Figure 4-6 are consistent with most polymerization occurring as homopolymerization in the water phase, there is a small but significant dependence of the rate on particle size, the rate increasing with decreasing particle size (increasing total surface area). This is consistent with small but significant amount of polymerization occurring as tethered chains and/or in the particle phase. The colloidal behavior provides indisputable evidence that significant hairy-layer grafting takes place, consistent with the dependence on size/surface area seen in Figure 4-6.

Another point of note in the data is seen in Figure 4-4 as that the heat flow, and hence the rate, is monotonically increasing until the initiator feed is switched off. If the redox initiator couple were to have a rapid reaction rate, so that the radical flux would rapidly assume a constant value, then the normal steady state rate observed in solution polymerization at low conversions would result. If classical free-radical polymerization kinetics were obeyed, this would give a ln[M] which is linearly dependent on time. However, if the value of the termination rate coefficient k_t (actually the termination rate coefficient averaged over all chain lengths, $<k_t>$) were to decrease significantly with conversion (which will occur because of chain-length-dependent termination (25, 51, 121)) then ln[M] would decrease faster than linearly with time. On the other hand, if the redox couple were to react slowly, then one would expect a more rapidly decreasing ln[M] during the TEPA feed, beyond any due to a decrease in k_t.

A decrease in k_t with conversion arises because termination in free-radical polymerization (beyond the glass transition) is dominated by diffusion of short chains (25, 51, 121). However, in the present system, this change in k_t would be very small over the range of conversion studied here, in which monomer is dilute and high conversion is not attained (initially [M] ~ 0.4 M, and [M] never falls below 0.3 M at the end of any TEPA feed), and the system does not gelatinize. Typical data for the termination rate coefficient in solution under such conditions (e.g. (121)) show that the change in k_t for our system will be negligible over this conversion range.

Given an essentially constant k_t, one would thus expect a ln[M] which would be linear in time if the redox couple were to establish a rapid steady state in radical flux. This expectation is contrary to what is seen in Figure 4-5, which implies that the radical concentration increases throughout the initiator feed period. The simplest explanation for this observation is that the redox couple reacts slowly.

4.2.3.1 Effect of Initiator Feed Rate

The evolution of the heat of reaction (proportional to the rate of reaction) is shown as a function of time for varying TEPA feed rates in Figure 4-4. It should be remembered that the exotherm seen in this plot is attributable to polymerization in the water, tethered-chain and particle phases. In all cases, Q_r steadily increases with TEPA feed and then decreases after the TEPA feed was stopped. To adjust for changes in monomer concentration with time, these curves have been replotted as follows. If one assumes that polymerization occurs only in the water and hairy-layers phases, and that the monomer concentration in the hairy layer is the same as in bulk water, then one can re-write eq 4-15 as:

$$R_p = -\frac{d[M]_w}{dt} = k_p\,[M]_w\,([R^\bullet]_w + [R^\bullet]_{hl}) = k_p\,[M]_w\,[R^\bullet]_{eq} \qquad (4\text{-}16)$$

Under this assumption, the equivalent total concentration of polymerizing radicals, $[R^\bullet]_{eq}$, can thus be estimated by plotting $-(d[M]_w/dt)/k_p[M]_w$, using the value of k_p for methyl methacrylate quoted above. Figure 4-7 shows the data so obtained as a function of time. If the redox couple attained a rapid steady state, then

$[R^\bullet]_{eq}$ should be independent of time; instead, the radical concentration climbs steadily. For reasons outlined above, this is unlikely to be due to a significant decrease in k_t over the course of these particular polymerizations.

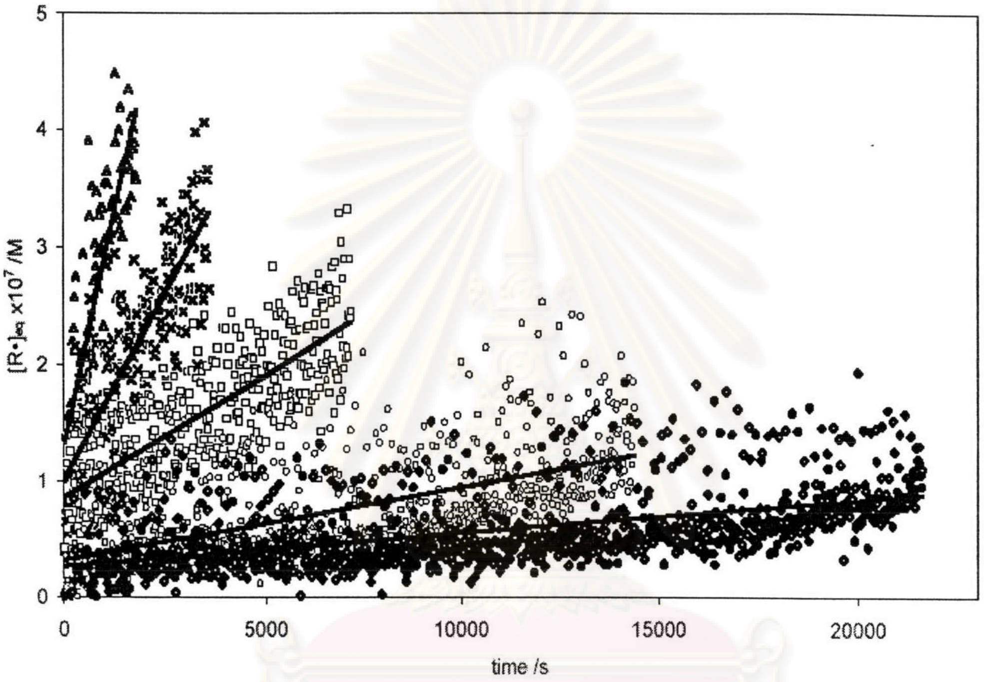

Figure 4-7 Equivalent total concentration of polymerizing radicals, $[R\bullet]_{eq}$, as a function of time for different TEPA feed times: (Δ) 0.5h, (×) 1h, (□) 2h, (□) 4h, and (◊) 6h.

The simplest explanation of this observation is that the rate at which the redox couple reacts is relatively slow, so that radical concentration climbs steadily with feed rate. The dependence of $d[R^\bullet]_{eq}/dt$ on the feed rate, i.e. of the reciprocal of the feed time t_f, is shown in Figure 4-8. For the more rapid feed rate, a doubling of feed rate produces a doubling of the polymerizing-radical generation rate, suggesting that bimolecular termination does not exert the very large kinetic influence it normally has in free-radical polymerizations. However, this is not as pronounced at the slow feed rates, where termination by chain transfer may become more important and the uncertainties in the calorimetric data are much greater. While all plots can be fit reasonably well by a linear dependence of d[R$^\bullet$]$_{eq}$/dt on feed rate, initial values of d[R$^\bullet$]$_{eq}$/dt are significantly higher.

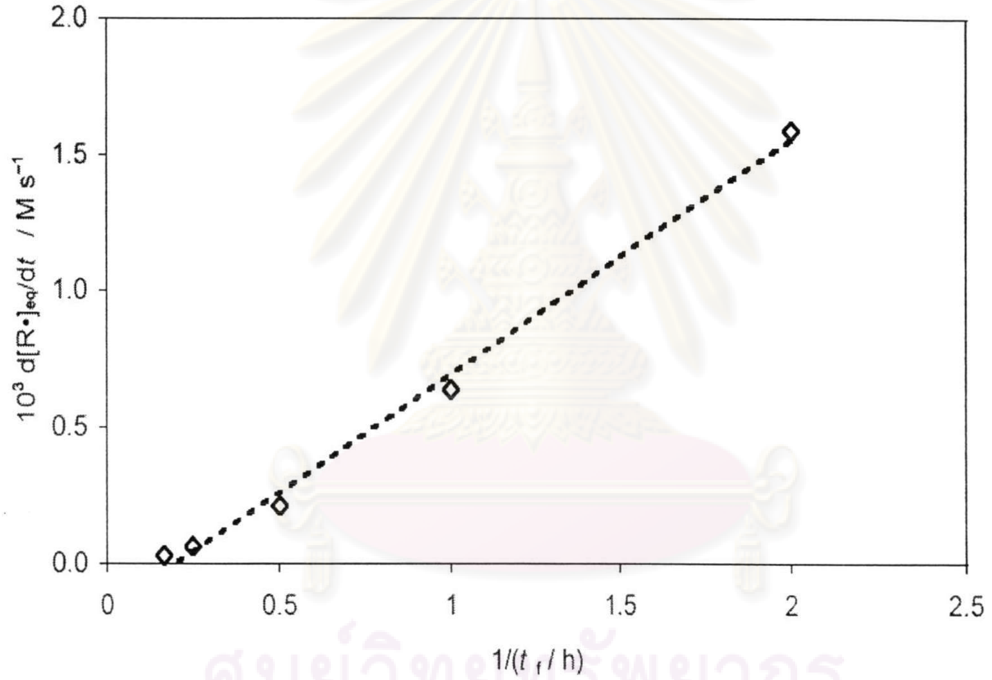

Figure 4-8 Derivative of the data of Figure 4-7, i.e., d[R•]$_{eq}$/dt, as a function of the feed rate, i.e. of the reciprocal of the TEPA feed time t_f.

This approximate linear dependence of the rate of generation of polymerizing radicals with total amount of initiator is consistent with a slow rate of reaction of the redox couple and a slow termination rate.

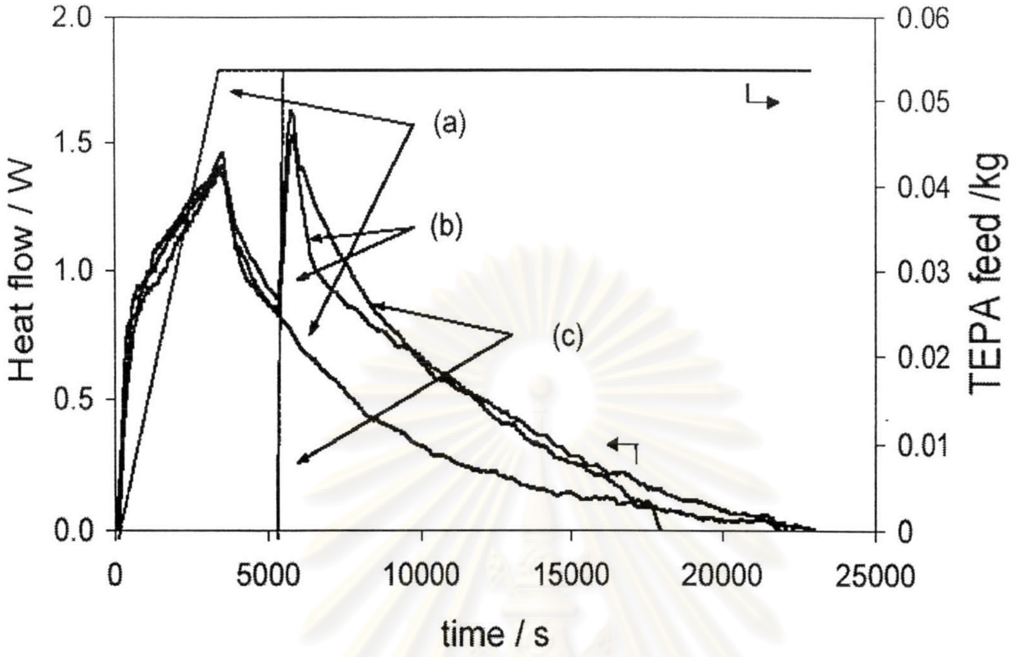

Figure 4-9 Heat flow during the grafting reaction of poly(DMAEMA) on polyisoprene after discontinuation of TEPA feed for 30 min (a) no addition, (b) adding H_2O and (c) adding *t*-BHP. The arrows for each data set show both Q_r and the corresponding feed profile.

In order to test the hypothesis that the free-radical decomposition of TEPA was slow on the timescale of the reaction due to a non-radical pathway in the aqueous phase, a more aqueous-soluble hydroperoxide (*t*-butyl hydroperoxide, *t*-BHP) was added 30 min after the TEPA feed period to confirm the existence of unreacted TEPA. When this was done, additional heat was generated, as shown in Figure 4-9. As the temperature of the feed (21–22°C) is warmer than the reaction temperature (15°C), the same measurement was carried out by feeding in the same quantity of pure water to see if the observed heat increase is simply a thermal artifact, as shown in Figure 4-9. The heat curves given by feeding *t*-BHP and a similar quantity of water are nearly identical, which suggests that the reaction of TEPA with CHP was relatively rapid and little TEPA remains in solution 30 min after the end of the initiator feed. An interpretation of these results will be given after consideration of the additional type of data the next section.

4.2.3.2 Rate after Initiator Feed Completed

The rate behavior after the initiator feed has been completed should in principle give information on the radical-loss processes in the system. In the present case, these data are not easy to interpret quantitatively, because the reaction between residual TEPA and CHP may be relatively slow, given the slow rate at which these species encounter in the interfacial phase. All that can be stated from the post-feed data in Figure 4-4 is that the radical-loss process is slow: of the order of 10^4 s. An explanation for this observation is given in the next section.

4.2.4 Inferences

Dynamic light scattering measurements are consistent with tethered poly (DMAEMA) chains being longest at highest radical flux, which is most readily explicable in terms of minimal influence of bimolecular termination. This inference, although consistent with the data, at first seems counter-intuitive: this is a redox-imitated system, and one would expect a high rate of termination of polymerizing radicals. However, further mechanistic inferences will show that this conclusion is in fact consistent with conventional precepts of free-radical polymerization.

All results are consistent with a model where the generation of tethered propagating radicals is a rare event. This involves encounter between the hydrophobic (CHP) and hydrophilic (TEPA) components of the redox couple meeting at the interface and forming a hydrophobic cumyloxyl radical. This must cause an abstraction reaction with an isoprene unit on the polymer at or near the interface, so that propagation with the hydrophilic monomer (DMAEMA) can commence. While this is the process which forms the hairy layer, it is not the dominant mode of polymerization, which is aqueous-phase homopolymerization of DMAEMA.

The rate data after TEPA feed has been stopped cannot be interpreted quantitatively (at least, until one can separate slow residual TEPA/CHP interactions from radical termination). It might tentatively be supposed that these data are semi-quantitatively in accord with the foregoing hypothesis. The most likely termination process is transfer to monomer to form a monomeric radical; this radical will then propagate in the water phase to form homopolymer, and eventually undergo termination with another such radical in the water phase. The fastest time for this radical loss process would be if such termination took place immediately after the transfer step, which would give a time-scale for termination of $(k_{\mathrm{tr}}\,[\mathrm{M}]_{\mathrm{w}})^{-1}$, where k_{tr} is the rate coefficient for transfer from the growing radical to monomer. There are no data for the transfer constant of DMAEMA, but the corresponding value for methyl methacrylate has been reported as $k_{\mathrm{tr}} = 10^{5.3} \exp(-45.9\ \mathrm{kJ\ mol^{-1}}/\,RT)\ \mathrm{dm^3\ mol^{-1}\ s^{-1}}$ (these Arrhenius parameters are re-processed from the original data (122), which were reported as $k_{\mathrm{tr}}/k_{\mathrm{p}}$, using the values of k_{p} for methyl methacrylate established by an IUPAC Working Party (100, 123)). Assuming the same value is applicable to

DMAEMA, and using the values of $[M]_W$ given Figure 4-5, yields a fastest radical-loss time $(k_{tr}[M]_W)^{-1}$ of 3.5×10^3 s. This is consistent with the observed timescale for the slowing in heat loss seen in Figure 4-4 of ~10^4 s. However, this predicts a high degree of polymerization for the chain: 10^5. The radius of gyration of such a chain can be primitively estimated from typical characteristic ratios as more than 10^2 nm. While this value is high, it is not impossible because the DLS data of Table 4-5 show that the hairy layer can extend as much as 50 nm into the water phase. The observed timescale for slow diminution of rate after switching off the initiator feed is thus likely to be a combination of relatively slow time for radical generation from the redox couple leading to a slow rate of creation of shorter radicals which contribute to the radical loss process by short-long termination, and the above-mentioned chain stoppage by (slow) transfer.

4.3 Grafting of Hydrophilic Polymers onto Natural rubber Latexes

From the previous section, the kinetics of grafting reaction of poly(DMAEMA) onto synthetic polyisoprene latexes were investigated. The results showed that while this topology-controlled" reaction is responsible for the formation of the hairy layer, the dominant polymerization process seems to be the formation of ungrafted poly (DMAEMA) in the water phase generated by chain transfer reaction.

The graft copolymerization of hydrophilic monomers, DMAEMA and DMAEA or HEMA, onto the natural rubber latex was also carried out in the second-stage emulsion polymerization using different redox initiator systems, CHP/TEPA, *t*-BHP/TEPA, and $K_2S_2O_8/K_2S_2O_5$. The reaction parameters such as monomer and initiator concentrations and reaction temperature on the conversion, grafting properties and some properties of the grafted copolymers were investigated.

4.3.1 Types of Redox Initiator on Grafting Reaction

Three redox initiator systems, CHP/TEPA, *t*-BHP/TEPA, and $K_2S_2O_8/K_2S_2O_5$ were used in the grafting copolymerization of hydrophilic monomers, DMAEMA, onto the hydrophobic polymer, natural rubber latex, to investigate the locus of polymerization. The percentage of conversion and grafting efficiency, and other graft performance of NR-*g*-DMAEMA copolymers are shown in Table 4-6 and Figure 4-10.

Table 4-6 Effect of redox initiator systems on the percentage of conversion and grafting efficiency, homopolymer and free NR of NR-*g*-P(DMAEMA) copolymers

Reaction Properties	$K_2S_2O_8/K_2S_2O_5$	*t*-BHP/TEPA	CHP/TEPA
Conversion (%)	62.6	57.5	47.8
Grafting efficiency (%)	33.1	45.3	52.0
Free homopolymer (%)	41.9	31.4	23.0
Free NR (%)	38.8	32.3	29.5

Reactions were carried out at 25°C for 24 h, DMAEMA = 15 phr, redox initiator systems $K_2S_2O_8/K_2S_2O_5$, *t*-BHP/TEPA and CHP/TEPA (1:1) = 0.5 phr.

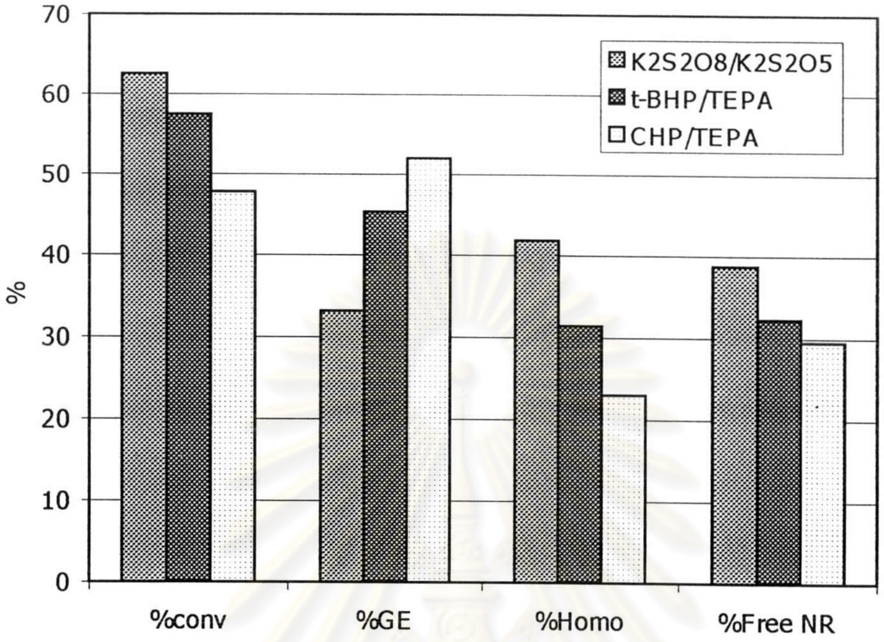

Figure 4-10 Effect of types of redox initiator systems on percentage of conversion, percentage of grafting efficiency, homopolymer and free NR.

Figure 4-10 shows the conversion, grafting efficiency, and grafting performance of NR-*g*-DMAEMA copolymers, using different types of initiator system, CHP/TEPA, *t*-BHP/TEPA, and $K_2S_2O_8/K_2S_2O_5$ when keeping the other parameters constant. It can be seen that CHP/TEPA gave the highest grafting efficiency and the smallest homopolymer content. The CHP/TEPA was concluded to be more effective than *t*-BHP/TEPA and $K_2S_2O_8/K_2S_2O_5$ for grafting DMAEMA onto natural rubber. This can be explained that the partitioning ability of CHP into natural rubber is higher than those of *t*-BHP and $K_2S_2O_8$ due to its hydrophobicity. The partitioning ability also affects to the locus of grafting reaction. It is expected that, for the CHP/TEPA system, the higher radical concentration could be found on the natural rubber surface than those in *t*-BHP/TEPA and $K_2S_2O_8/K_2S_2O_5$ systems. On the other hand, because *t*-BHP is partially soluble in both organic and aqueous phase and $K_2S_2O_8/K_2S_2O_5$ is only soluble in aqueous phase, the radicals are mostly generated in the aqueous phase. This leads to a higher grafting efficiency in CHP/TEPA and a smaller homopolymer content than those in *t*-BHP/TEPA and $K_2S_2O_8/K_2S_2O_5$, respectively.

4.3.2 Gel Content Analysis

A useful qualitative measure to indicate grafting and/or crosslinking reaction is the gel fraction. The natural rubber latex used here has a gel content of 48.8%. One should be careful when using the gel content data to compare results in the literature, because gel content analysis is technique-dependent. Therefore, the gel content analysis data was used for comparing with other modified latexes synthesized in this work. Because some gelation may arise entirely through the natural rubber chains crosslinking between them due to the presence of the initiator, comparison must also be made with natural rubber latex which has been exposed to radicals in the absence of any added monomer. The rate of producing primary radicals (k_d) of CHP is higher than that of *t*-BHP. (k_d of CHP is 1.7×10^{-6} s^{-1} in benzene at 130°C and k_d of *t*-BHP is 3×10^{-7} s^{-1} in benzene at 130°C (108)).

Table 4-7 Gel content and degree of swelling for cast films of NR, self crosslinked NR, and NR-*g*-P(DMAEMA)

Sample	Gel Content (%)	Degree of Swelling (swollen wt/initial wt)
NR	48.8	28.7
NR/CHP-TEPA	93.4	12.3
NR/*t*-BHP-TEPA	90.6	14.7
NR/$K_2S_2O_8$-$K_2S_2O_5$	41.7	20.9
NR-*blend*-P(DMAEMA)	46.5	27.5
NR-*g*-P(DMAEMA)/CHP-TEPA	76.7	20.5
NR-*g*-P(DMAEMA)/*t*-BHP-TEPA	71.5	22.2
NR-*g*-P(DMAEMA)/$K_2S_2O_8$-$K_2S_2O_5$	62.9	24.9

The results obtained for the gel content and degree of swelling of natural rubber, natural rubber crosslinked by initiators and NR-*g*-P(DMAEMA) are summarized in Table 4-7. For all cases, the gel content is greater for polymers with a smaller swelling ratio. For both the pure NR film and NR-*blend*-P(DMAEMA), the gel content is about 46.5%, and the swelling ratio is large, where NR films crosslinked by the redox initiators in the absence of monomer have a range of the gel content of 41.7–93.4% and a smaller swelling ratio. All NR-*g*-P(DMAEMA) films show characteristics between these two extreme cases, with gel contents of 62.9–76.7% and the intermediate swelling ratios. As shown in Table 4-7, the gel content of the graft copolymer prepared by CHP/TEPA is larger than that by *t*-BHP/TEPA and

$K_2S_2O_8/K_2S_2O_5$, respectively. This confirms that the initiating radicals are generated on the surface of natural rubber particles when using the CHP/TEPA system due to its partitioning ability.

4.3.3 Effect of Monomer Concentration

In this work, the natural rubber latex containing the polymer backbone of *cis*-1,4-polyisoprene was used as the seed particle for grafting reaction. DMAEA, DMAEMA and HEMA monomers were each added as the grafting monomers to polymerize with the polymer backbone. The effects of monomer concentrations on the percentage of conversion and grafting properties, grafting efficiency and percentage of homopolymer and free NR were investigated using the monomer concentration in the range of 5–20 phr and keeping the concentrations of other reagents constant.

The effects of monomer concentration of both DMAEA and DMAEMA on the percentage of conversion and grafting properties are shown in Table 4-8 and Figures 4-11–4-14. As seen from the Figures 4-11 and 4-13, the percentage of conversion increases with increasing both monomer concentrations, In Figures 4-11 and 4-13, the grafting efficiency increases at the lower concentration range of monomers, reaches a maximum at the monomer concentration of 15 phr and then decreases with further increase of the concentration.

The increase in the grafting efficiency might be due to the complexion of rubber with monomers, which is favored at high monomer concentration and gel effect. An increase in the viscosity of the reaction medium due to the solubility of poly (DMAEA) and poly(DMAEMA) in the aqueous phase would be more pronounced at higher monomer concentration. The decrease in grafting efficiency after 15 phr may be caused by the higher monomer concentrations, many reactions completing with grafting probably take place in solution at the same time, i.e. combination and disproportionation of poly(DMAEA) and poly(DMAEMA) macroradicals. When the concentrations of poly(DMAEA) and poly(DMAEMA) macroradicals increase, the rates of their combination and disproportionation increase more quickly than the grafting rate with the rubber macroradicals. On the other hand, the rate of monomer diffusion is bound to be progressively affected in the polymer formed, which of course it grows most rapidly when high concentrations of monomer are used.

In Table 4-8 the effects of monomer type on conversion and grafting performance are presented. It was found that the conversion and grafting efficiency in case of DMAEMA monomer are smaller than that of DMAEA. This decrease may be probably be due to the poorer accessibility of the DMAEMA monomers to the macroradical centers on the natural rubber backbone because of the enhancement of the steric hindrance caused by the increase in the methyl group.

Table 4-8 Effect of the monomer concentration on the properties of graft copolymers; initiator concentration 0.5 phr, reaction temperature 25°C, and reaction time 24 h

Reaction Properties	DMAEA				DMAEMA			
	Monomer Concentration (phr)				Monomer Concentration (phr)			
	5	10	15	20	5	10	15	20
Solid Content (%)	28.1	28.9	30.0	31.9	28.0	28.4	29.4	30.6
Conversion (%)	35.4	46.1	55.1	68.3	30.8	36.4	47.8	55.3
Grafting Efficiency (%)	25.7	50.8	60.2	52.0	20.5	32.9	52.0	47.9
Free NR (%)	39.4	31.0	27.0	20.6	43.0	29.1	29.5	25.4
Free Homopolymer (%)	26.3	22.7	21.9	32.8	24.5	24.4	23.0	28.8
Water absorption (%)	15.4	17.9	18.2	19.1	14.8	16.2	17.9	18.9
Contact angle (degree)	96.9	89.7	80.5	78.9	98.7	88.4	84.7	81.8
Stability at low pH	+	+ +	+ +	+ +	+	+ +	+ +	+ +

+ = partly coagulated; and + + = stable.

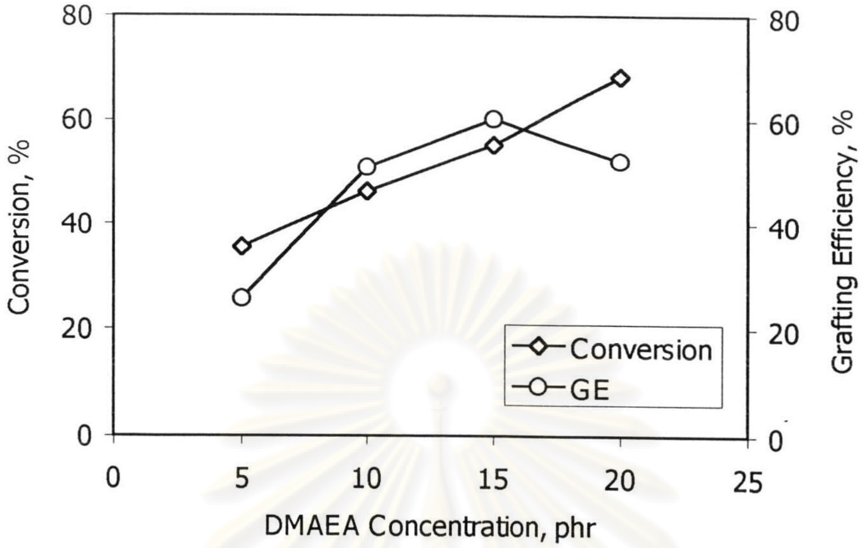

Figure 4-11 Effect of DMAEA concentration on the percentage conversion and grafting efficiency at 25°C, initiator concentration 0.5 phr, and reaction time 24 h.

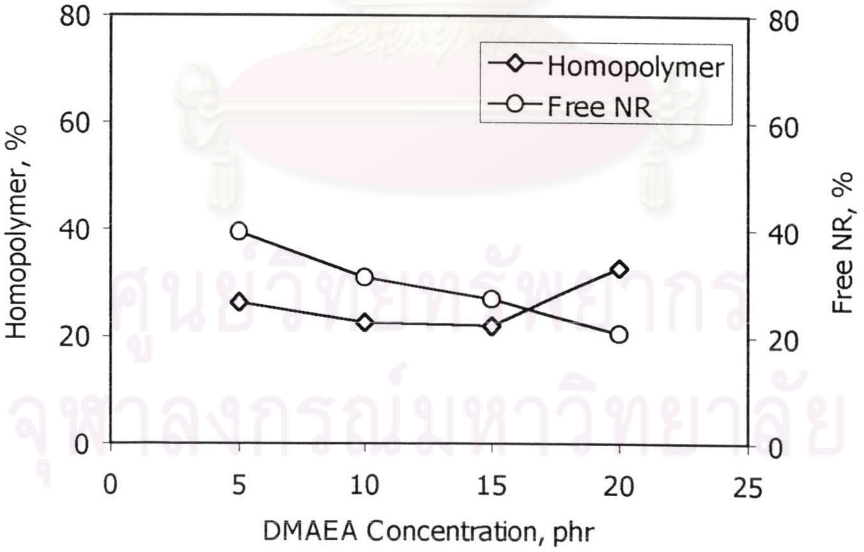

Figure 4-12 Effect of DMAEA concentration on the percentage of homopolymer and free NR at 25°C, initiator concentration 0.5 phr, and reaction time 24 h.

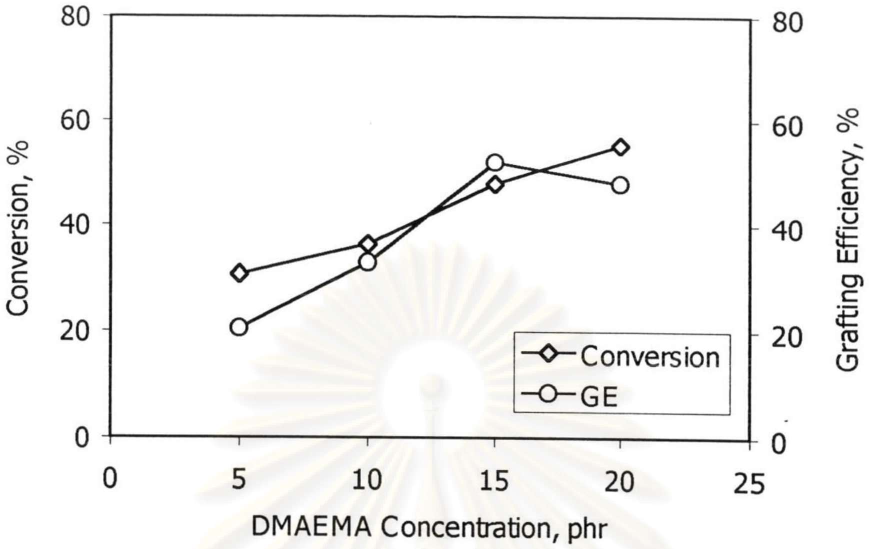

Figure 4-13 Effect of DMAEMA concentration on the percentage conversion and grafting efficiency at 25°C, initiator concentration 0.5 phr, and reaction time 24 h.

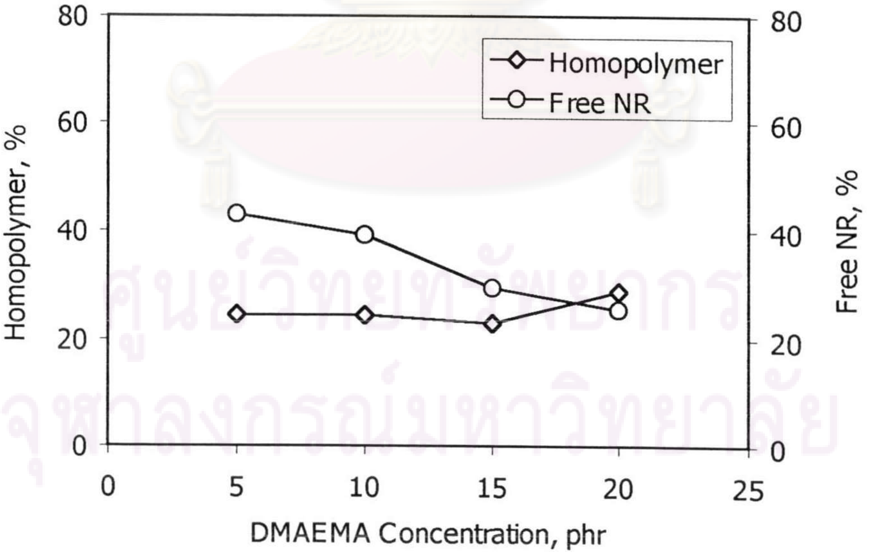

Figure 4-14 Effect of DMAEMA concentration on the percentage of homopolymer and free NR at 25°C, initiator concentration 0.5 phr, and reaction time 24 h.

The effect of monomer concentration on the water absorption behavior and contact angle was shown in Table 4-8. It was found that the water absorption increases with increasing the monomer content. While the contact angle of unmodified natural rubber is about 100°, the contact angle of modified natural rubber films decreases correspondingly upon increasing the monomer content, implying that higher hydrophilicity was achieved with increasing monomers.

Generally natural rubber latex particles are believed to be stabilized by the presence on their surfaces of adsorbed carboxylic anions from fatty acid soaps or protein molecules, or both. The adsorbed anions cause the particle surface to have a net negative electrical charge, which produces inter-particle repulsive forces and ensures absence of aggregation. The reduction in pH produced by the addition of acids to latex, affects destabilization by reducing the ionization of the adsorbed materials and diminishing the interparticle repulsive potential to less than *kT*, the energy due to Brownian motion. Table 4-8 also shows the stability of modified natural rubber at low pH increases with increasing the monomer concentration used for grafting. While the unmodified natural rubber latex is colloidally unstable at low pH, grafted latexes prepared were stable. The stability at low pH increases when increasing the monomer content which grafted on the surface of the rubber particles can be due to the protonation of the amino groups increased.

4.3.4 Effect of Initiator Concentration

The effect of the amount of initiator on the percentage of conversion and grafting efficiency of two monomers, DMAEA and DMAEMA on natural rubber latex was studied over the range of approximately 0.1–1.0 phr while keeping the concentrations of all other reagents constant. The percentages of conversion and grafting efficiency are shown in Table 4-9 and Figures 4-15 and 4-17. As the amount of initiator increased, more radicals are produced; consequently, this increases the number of grafting sites, which results in higher grafting efficiency.

The grafting efficiency was seen to increase with an increase in the amount of initiator from 0.1 to 1.0 phr for both monomers (Figures 4-15 and 4-17). This trend can be explained by the fact that the radicals transfer to either rubber or monomer, producing macroradicals, which is enhanced by increasing the initiator concentrations, thus resulting in an increase in grafting. However, beyond the amount of 0.5 phr, the grafting efficiency decreases, which results from the increasing conversion of free homopolymer over 0.5 phr. Under this condition, the length of grafted chains can hardly anything to do with the free polymer radicals. The excessive free polymer radicals then react with each other to form a greater amount of the free homopolymers rather than graft on the natural rubber radicals and the length of the grafted chains thus decreases. Therefore, the formation of the free polymer is greatly promoted at high initiator content (Figures 4-16 and 4-18). On the other hand, the probability for the rate of chain transfer for the free polymer radicals to the natural rubber backbone is

Table 4-9 Effect of the initiator concentrations on the properties of graft copolymers; monomer concentration 15 phr, reaction temperature 25°C, and reaction time 24 h

Reaction Properties	DMAEA				DMAEMA			
	Initiator Concentration (phr)				Initiator Concentration (phr)			
	0.1	0.25	0.5	1.0	0.1	0.25	0.5	1.0
Solid content (%)	28.7	29.4	30.0	30.5	28.3	29.2	29.4	29.7
Conversion (%)	36.2	46.5	55.1	66.0	30.0	43.4	47.8	55.1
Grafting efficiency (%)	23.3	46.1	60.2	55.1	25.7	42.4	52.0	50.1
Free NR (%)	45.3	36.0	27.0	22.7	40.9	43.2	29.5	27.8
Free homopolymer (%)	27.8	25.1	21.9	29.6	23.8	25.0	23.0	27.5
Water absorption (%)	22.7	19.5	18.2	21.3	21.8	18.6	17.9	20.1
Contact angle (degree)	94.5	88.1	80.5	79.6	97.9	89.6	84.7	82.6
Stability at low pH	+	+ +	+ +	+ +	+	+ +	+ +	+ +

+ = partly coagulated; and + + = stable.

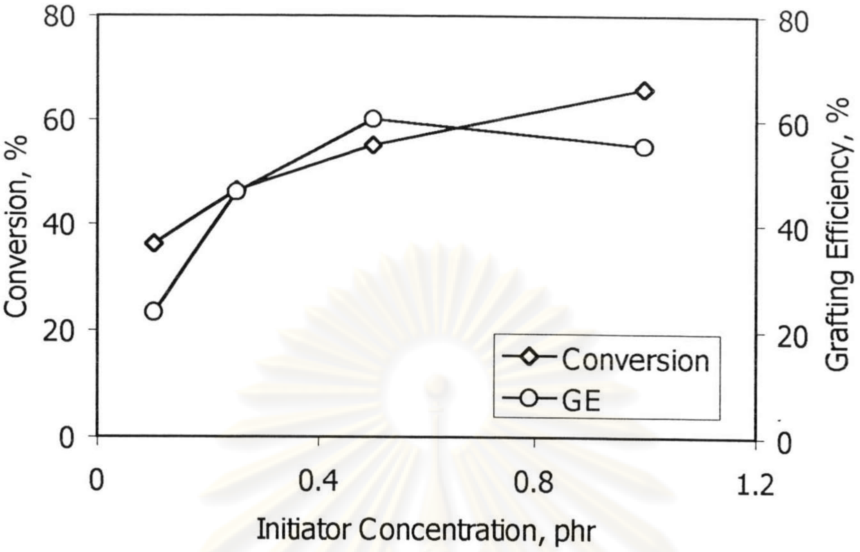

Figure 4-15 Effect of the initiator concentration on the percentage conversion and grafting efficiency at 25°C, DMAEA monomer concentration 15 phr, and reaction time 24 h.

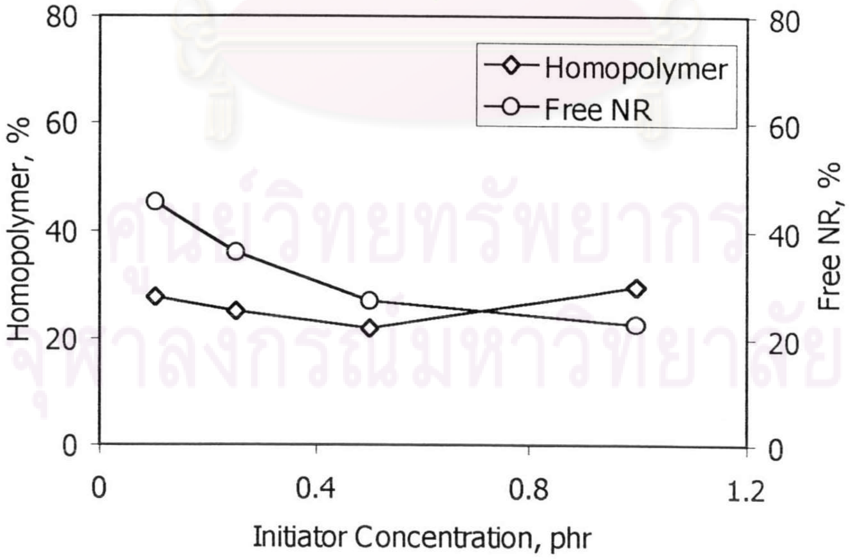

Figure 4-16 Effect of the initiator concentration on the percentage of homopolymer and free NR at 25°C, DMAEA monomer concentration 15 phr, and reaction time 24 h.

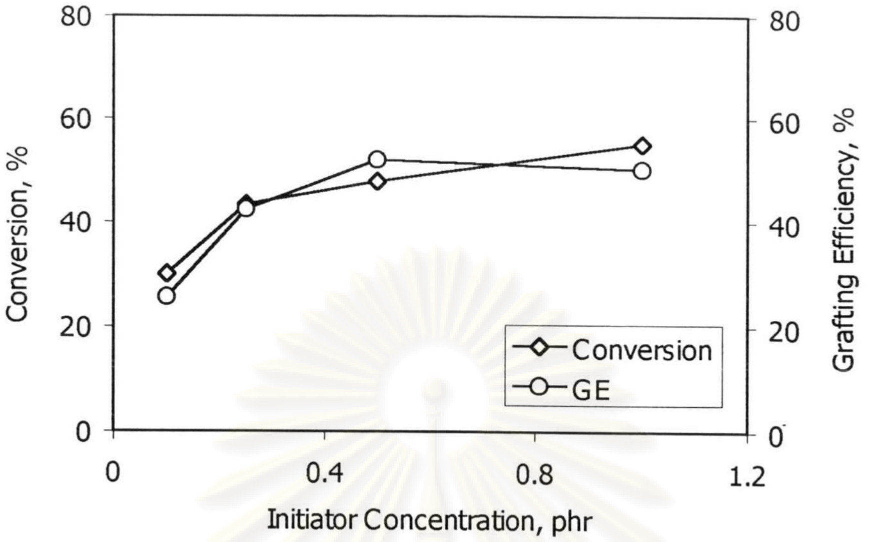

Figure 4-17 Effect of the initiator concentration on the percentage conversion and grafting efficiency at 25°C, DMAEMA monomer concentration 15 phr, and reaction time 24 h.

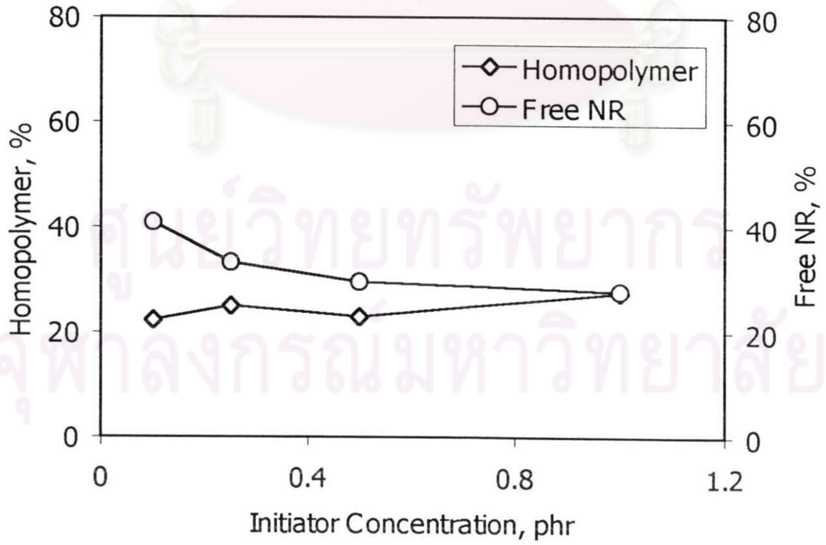

Figure 4-18 Effect of the initiator concentration on the percentage of homopolymer and free NR at 25°C, DMAEMA monomer concentration 15 phr, and reaction time 24 h.

less than the rate of termination of free polymer radicals, favoring the termination process of copolymers over the chain-transfer process. Similar results were also reported by Lenka et al. (87) and Ararapranee et al. (124) in the case of grafting methyl methacrylate onto natural rubber.

Table 4-9 shows the effect of initiator concentration on the water absorption and the surface contact angle of modified NR films. It was found that the contact angle of the films decreases with increasing the initiator concentration. This can be attributed to the fact that the NR films with a more hydrophobic were grafted by a more hydrophilic group in the second polymer. However, the water absorption of the modified NR film decreased initially and then subsequently increased with increasing the initiator concentration. The initial decrease was due to increase in the crosslink density of the rubber while the subsequent increase was due to increase in the hydrophilic content in the copolymer. In addition, the increase of the latex stability at low pH when the initiator content increases is also shown in Table 4-9.

4.3.5 Effect of Reaction Temperature

The graft copolymerizations of DMAEA and DMAEMA were carried out at four reaction temperatures between 15 and 30°C while keeping the concentrations of other reaction parameters constant. From Table 4-10 and Figures 4-19 and 4-21, it can be seen that the higher reaction temperature usually produces the greater conversion because more radicals are generated to consume monomer molecules.

Table 4-10 Effect of the reaction temperature on the properties of graft copolymers; monomer concentration 15 phr, initiator concentration 0.5 phr, and reaction time 24 h

Reaction Properties	DMAEA				DMAEMA			
	Reaction Temperature (°C)				Reaction Temperature (°C)			
	15	20	25	30	15	20	25	30
Solid content (%)	29.6	29.8	30.0	30.4	29.0	29.5	29.4	30.2
Conversion (%)	49.7	53.0	55.2	60.5	41.7	49.1	47.8	58.5
Grafting efficiency (%)	55.5	57.0	60.2	55.1	41.9	48.0	52.0	49.7
Free NR (%)	30.4	29.1	27.0	20.2	35.7	27.2	29.5	25.3
Free homopolymer (%)	22.1	22.8	22.0	27.1	24.2	25.5	23.0	29.4
Water absorption (%)	22.4	19.8	18.2	17.7	20.5	19.1	17.9	15.5
Contact angle (degree)	79.5	81.6	80.5	81.8	84.9	83.6	84.7	83.2
Stability at low pH	+ +	+ +	+ +	+ +	+ +	+ +	+ +	+ +

+ = partly coagulated; and + + = stable.

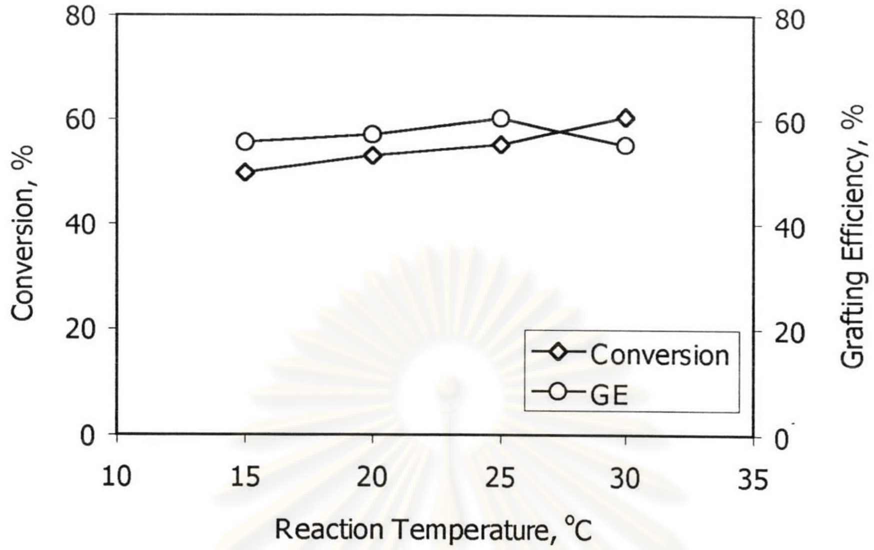

Figure 4-19 Effect of reaction temperature on the percentage conversion and grafting efficiency, DMAEA concentration 15 phr, initiator concentration 0.5 phr, and reaction time 24 h.

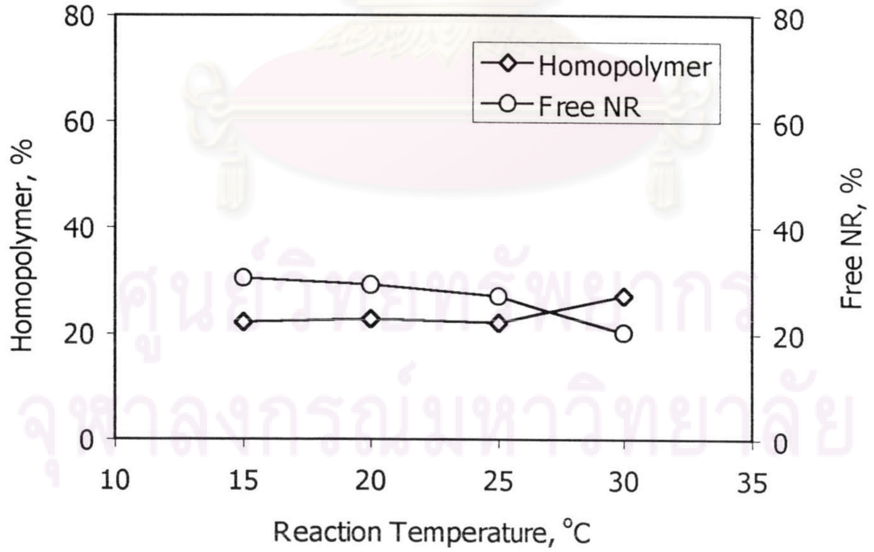

Figure 4-20 Effect of reaction temperature on the percentage of homopolymer and free NR, DMAEA concentration 15 phr, initiator concentration 0.5 phr, and reaction time 24 h.

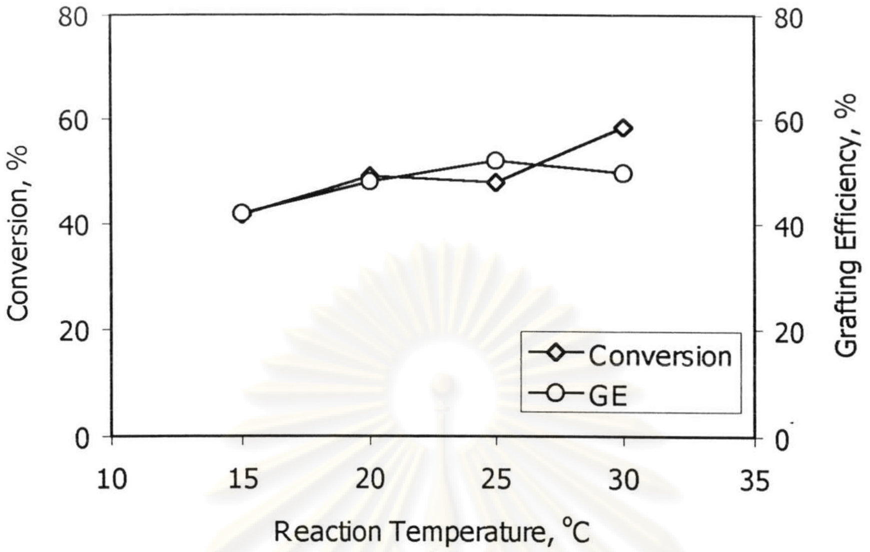

Figure 4-21 Effect of reaction temperature on the percentage conversion and grafting efficiency, DMAEMA concentration 15 phr, initiator concentration 0.5 phr, and reaction time 24 h.

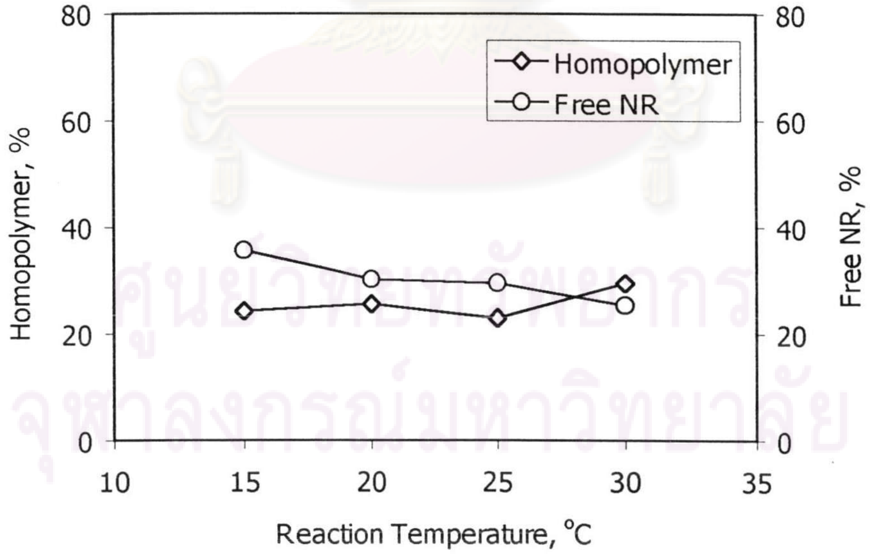

Figure 4-22 Effect of reaction temperature on the percentage of homopolymer and free NR, DMAEMA concentration 15 phr, initiator concentration 0.5 phr, and reaction time 24 h.

The decomposition rate of the initiators (CHP and *t*-BHP) depends on the reaction temperature. With increasing in the reaction temperature, more alkyloxyl radicals are produced. It is also known that the transfer of alkyloxyl radicals to rubber chain produces the graft copolymers. So, the perusal of the results indicates that the grafting efficiency increases as the polymerization temperature is increased up to 25°C (Figures 4-19 and 4-21). Then the grafting efficiency decreases with further increase in reaction temperature. The very rapid decomposition of the initiator yields an instantaneously high radical concentration and the radicals then might be acting as radical scavengers, which results in decreasing the initiator amount. Thus the result is a lower initiator efficiency which, however, fails to produce both the corresponding ungrafted homopolymer and graft copolymers.

In addition, another possibility to lead the grafting efficiency decreases with increasing the reaction temperature could be caused by the nature of the grafting monomers. Because the polymers of DMAEA and DMAEMA used are temperature sensitive, which phase transition could occur when the reacting temperature reaches above the lower critical solution temperature, LCST. This reason supports the use of the redox initiator, which can initiate the polymerization at low temperatures. The temperature which the phase transition occurred for poly(DMAEA) and poly (DMAEMA) at about 40°C in water (101).

The effect of the reaction temperature of the grafting reaction on the water absorption and the contact angle of modified NR films is revealed in Table 4-10. The monomer concentration and initiator concentration have been fixed at 15 phr and 0.5

phr, respectively for all latexes. The water absorption and contact angle of the graft-modified NR films were not significantly different when the reaction temperature was increased.

4.3.6 Modification of NRL by Grafting with HEMA Hydrophilic Monomer

This work is also an investigation of the modification of natural rubber (NR) by graft copolymerization of hydroxyethyl methacrylate (HEMA) in NR latex.

Table 4-11 Product appearance of graft copolymerization of HEMA on NRL

Run	HEMA (phr)	Product appearance
HE01	5.0	Aggregated
HE02	10.0	Paste formed

The reactions were carried out at 25°C, initiator concentration 0.5 phr.

The graft copolymerization of HEMA onto natural rubber latex was carried out using the redox initiator system (CHP:TEPA) similar to that of the DMAMEA monomer system. The second-stage polymerization of HEMA onto NR particles was carried out using the recipes presented in Table 3-5. It was found that coagulation occurred during the polymerization in all cases even in the presence of SDS (5 phr). As presented in Table 4-11 that at 5 phr of HEMA monomer the resulting latex aggregated, and when increasing the monomer concentration up to 10 phr the paste mass of the latex was formed at the earlier stage of the grafting reaction. It is shown that when increasing HEMA concentration, the non-ionogenic hydrophilic monomer caused the stability of the graft product to decrease. It can be explained that HEMA may act as dehydrating agent. It was thought that the graft copolymers themselves would enhance latex stability. However, the grafted polymers appeared to destabilize the latex in the sense that the modified NR latex was not macroscopically homogeneously stable. It is not clear how such a creaming process occurs. Nonetheless, it might be attributed to the insolubility of the polymer units bound to the NR. Similarly, poly(HEMA) can possibly form cross-particle bridging to result in flocculation.

In the later stage of the investigation of the effect of the added monomers to NR latex, it was observed that, at the small levels of added HEMA (2–4 phr) without initiator, the latex partly coagulated overnight. This observation strongly suggested that the HEMA monomer act as a de-stabilizer for NR latex. There are two possible explanations for the destabilization of the latex: First, the monomer is hydrophilic in nature, and can reduce the extent of the hydration layer at the surface of the rubber particles, thereby reducing the stability of the latex. Second, the monomer might react with the indigenous stabilizers of the latex, such as proteinaceous substances and fatty-acid anions, although it is difficult to suggest mechanisms for such reactions.

Minoura (125) investigated the effect of various lengths of the alkyl group of an alcohol, i.e., methanol, ethanol, and propanol, the functional group and molecular length of which are somewhat similar to the HEMA monomer molecule, upon the stability of NR latex. At low alcohol concentrations, the stability of the latex increased progressively with increasing amount of added alcohol. However, at certain levels of added alcohol, the alcohols are no longer able to increase the stability of the latex. In this study, the effect of the non-ionogenic hydrophilic monomers containing an –OH group upon the stability was studied. This strongly suggests that the monomer rapidly adsorbed on to the particle surfaces, perhaps bringing about a thickening of the adsorbed layers, possibly contributing to steric stabilization, and enhancing hydration. One would expect that the ethylenic groups of the monomers are more likely adsorb on to the surface of the particles than the hydroxyl groups, which would tend to remain in the aqueous phase. There is also the possibility that the monomer might become associated with the surface layers through hydrogen bonding involving the OH groups.

4.3.7 Functional Groups in the Grafted Natural Rubber

The existence of the grafting was first confirmed by observing the difference between the FT-IR spectra of natural rubber and the graft copolymers. The FT-IR spectra of natural rubber and the graft copolymers were recorded on a Perkin-Elmer FT-IR Spectrometer 1760. The spectra of natural rubber, NR-*g*-poly(DMAEA), and NR-*g*-poly(DMAEMA) are revealed in Figures 4-23 to 4-25, respectively.

From the FT-IR spectra, we found that the spectrum of pure natural rubber (Figure 4-23) is characterized by the presence of absorbance peaks attributed to the unsaturated carbon-carbon double bonds associated with the polyisoprene molecules. Some of these functional groups of grafted natural rubber are given in Table 4-12.

The spectra of NR-*g*-poly(DMAEA) (Figure 4-24) and NR-*g*-poly(DMAEMA) (Figure 4-25) show not only the characteristic natural rubber peaks, but also the additional absorption peaks of the carboxylic ester carbonyl group (C=O) stretching vibration at 1730 cm^{-1} and C-O-C stretching vibration at 1160 cm^{-1} of poly(DMAEA) and poly(DMAEMA). This indicates that the graft copolymer contains the DMAEA and DMAEMA chain structure.

Table 4-12 Absorbance peaks and corresponding functional groups determined by FT-IR spectroscopy of grafted natural rubber

Wavenumber, cm^{-1}	Assignment of functional group
834 (m)	C=C wagging
1375 (m)	C–H bending of CH_3
1450 (m)	C–H bending of CH_2
1662 (v)	C=C stretching
1730 (s)	C=O stretching
1160 (s)	C-O-C stretching
2852; 2960 (s)	C–H stretching of alkane
3036 (m)	=C–H stretching of alkene

s = strong, m = medium, w = weak, v = variable.

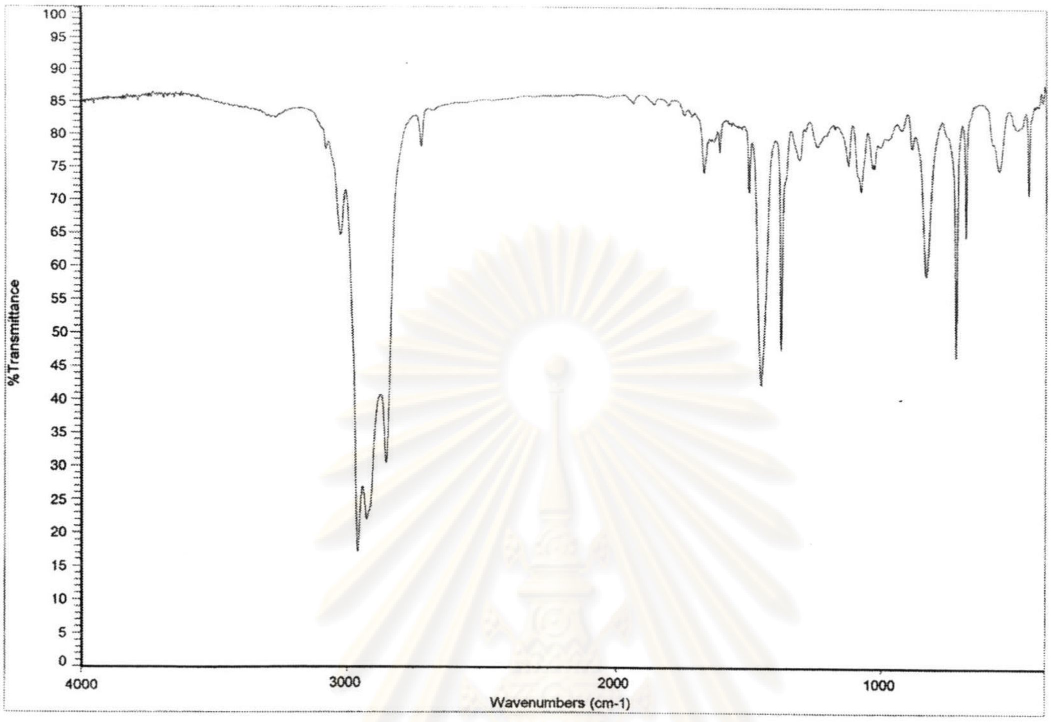

Figure 4-23 FT-IR spectrum of natural rubber.

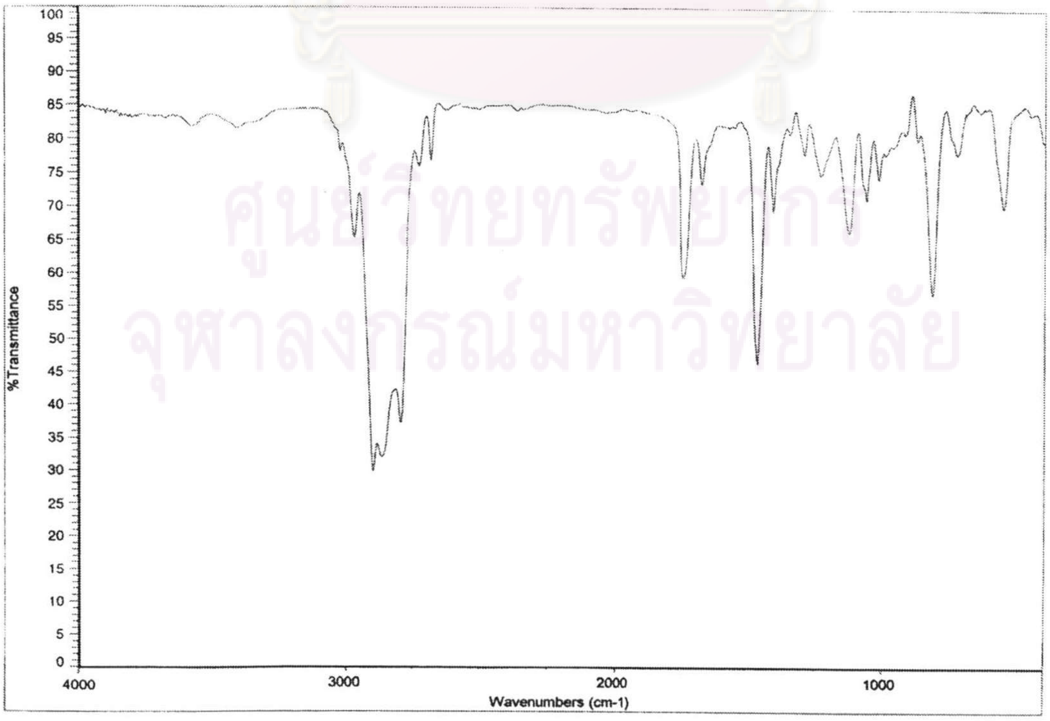

Figure 4-24 FT-IR spectrum of NR-*g*-poly(DMAEA).

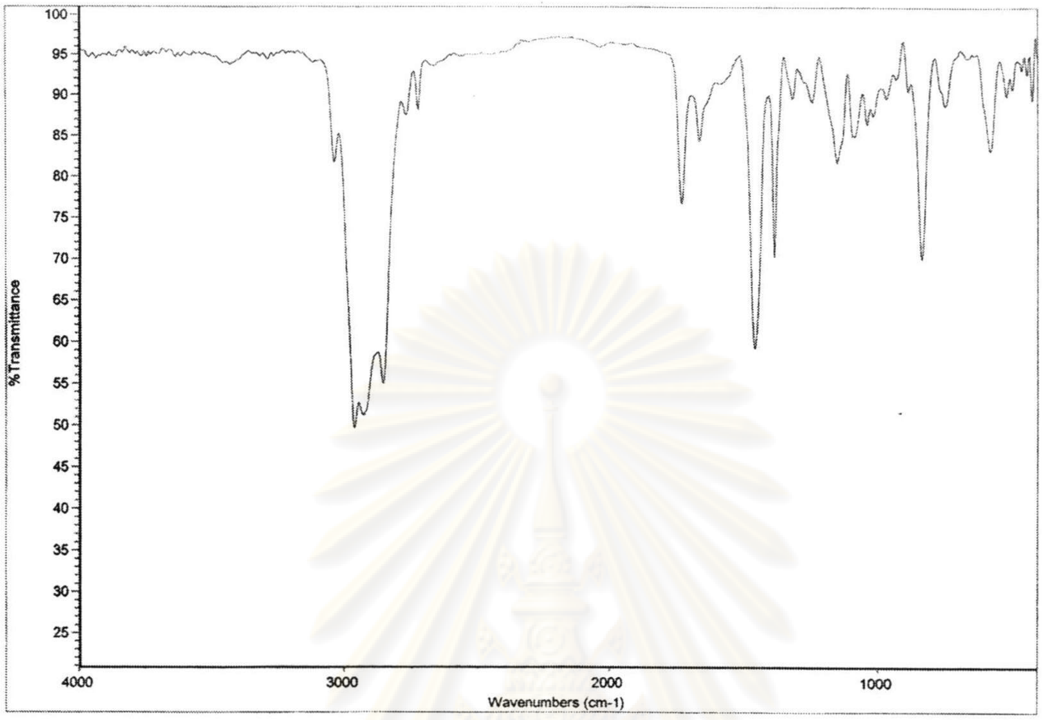

Figure 4-25 FT-IR spectrum of NR-*g*-poly(DMAEMA).

4.3.8 Morphological Observations by TEM

Figures 4-26–4-28 show transmission electron micrographs of natural rubber and grafted natural rubber particles of poly(DMAEMA) with 20 wt% of DMAEMA prepared using the CHP/TEPA redox initiator system. These particles were stained with osmium tetroxide (OsO_4) and phosphotungstic acid (PTA). Because OsO_4 can only stain the polyisoprene regions through reactions with the residual double bonds present in natural rubber, the darker areas therefore indicate the NR core regions, while the lighter areas are for poly(DMAEMA) film as the shell. Figure 4-26 shows that the NR latex particle are spherical in nature with a smooth surface. The NR latex particles covered with poly(DMAEMA) revealed irregular shapes,

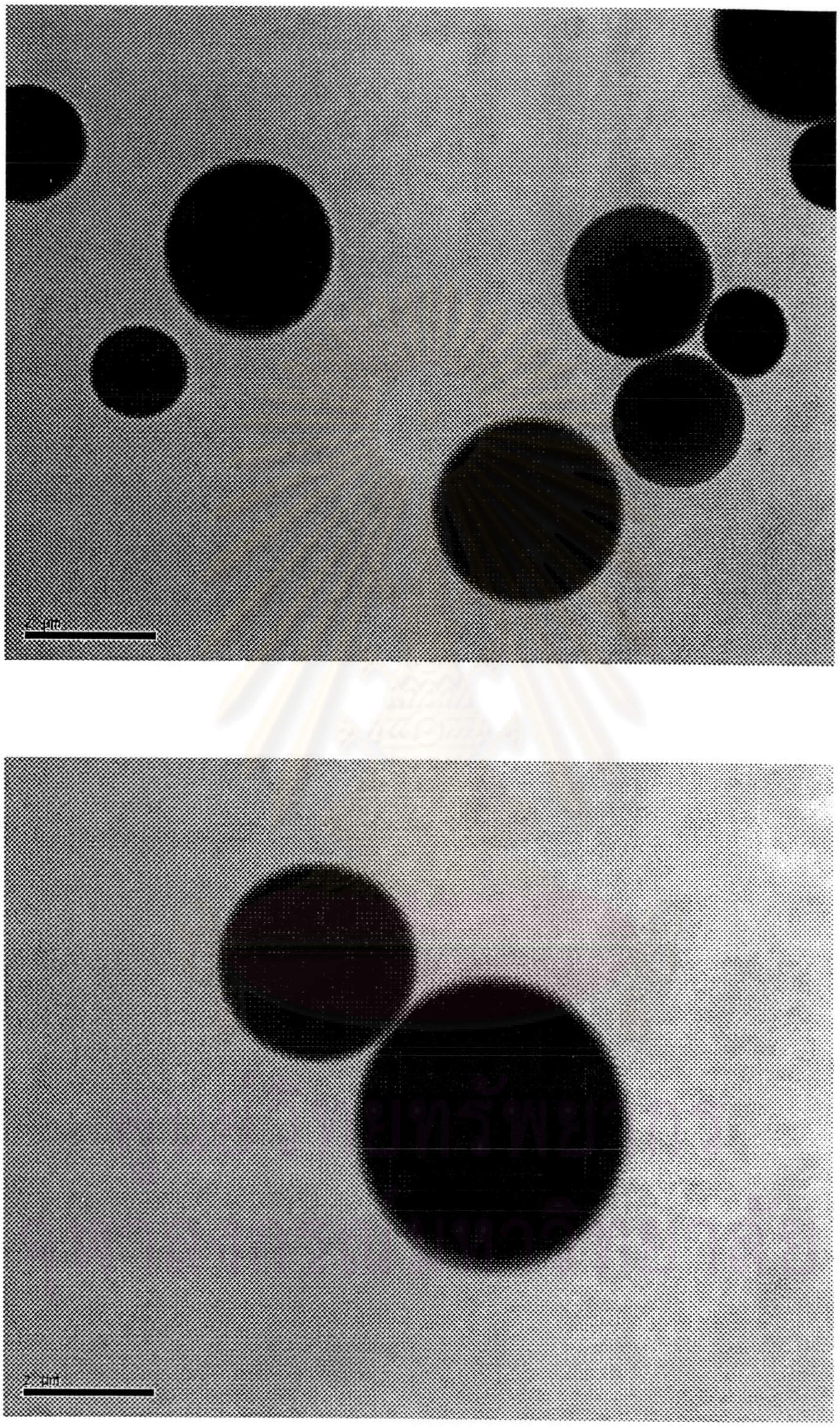

Figure 4-26 Transmission electron micrographs of natural rubber latex particles stained with 2% osmium tetroxide (OsO_4); bar is for 2 μm.

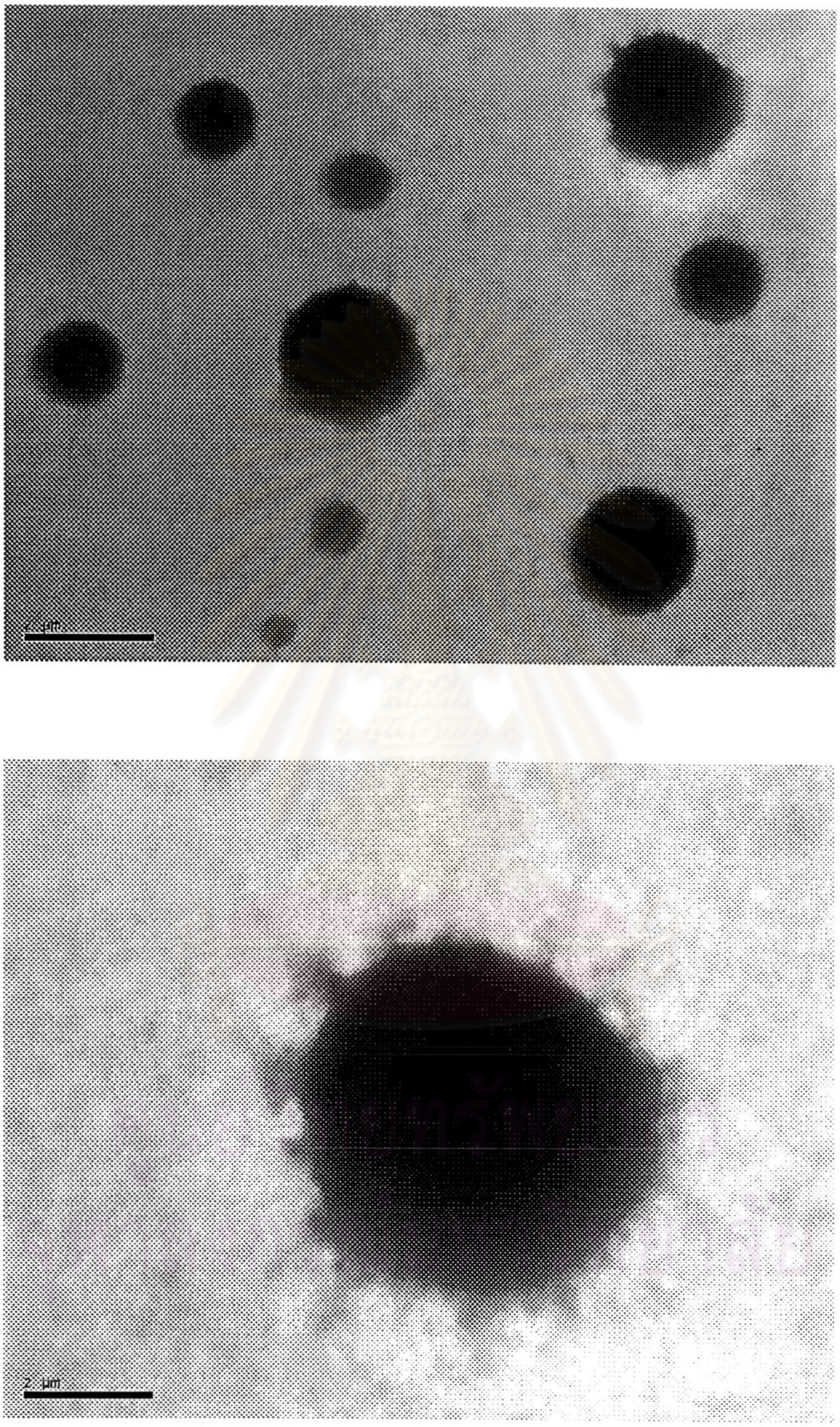

Figure 4-27 Transmission electron micrographs of NR-*g*-poly(DMAEA) latex particles positively stained with 2% osmium tetroxide (OsO_4); bar is for 2 μm.

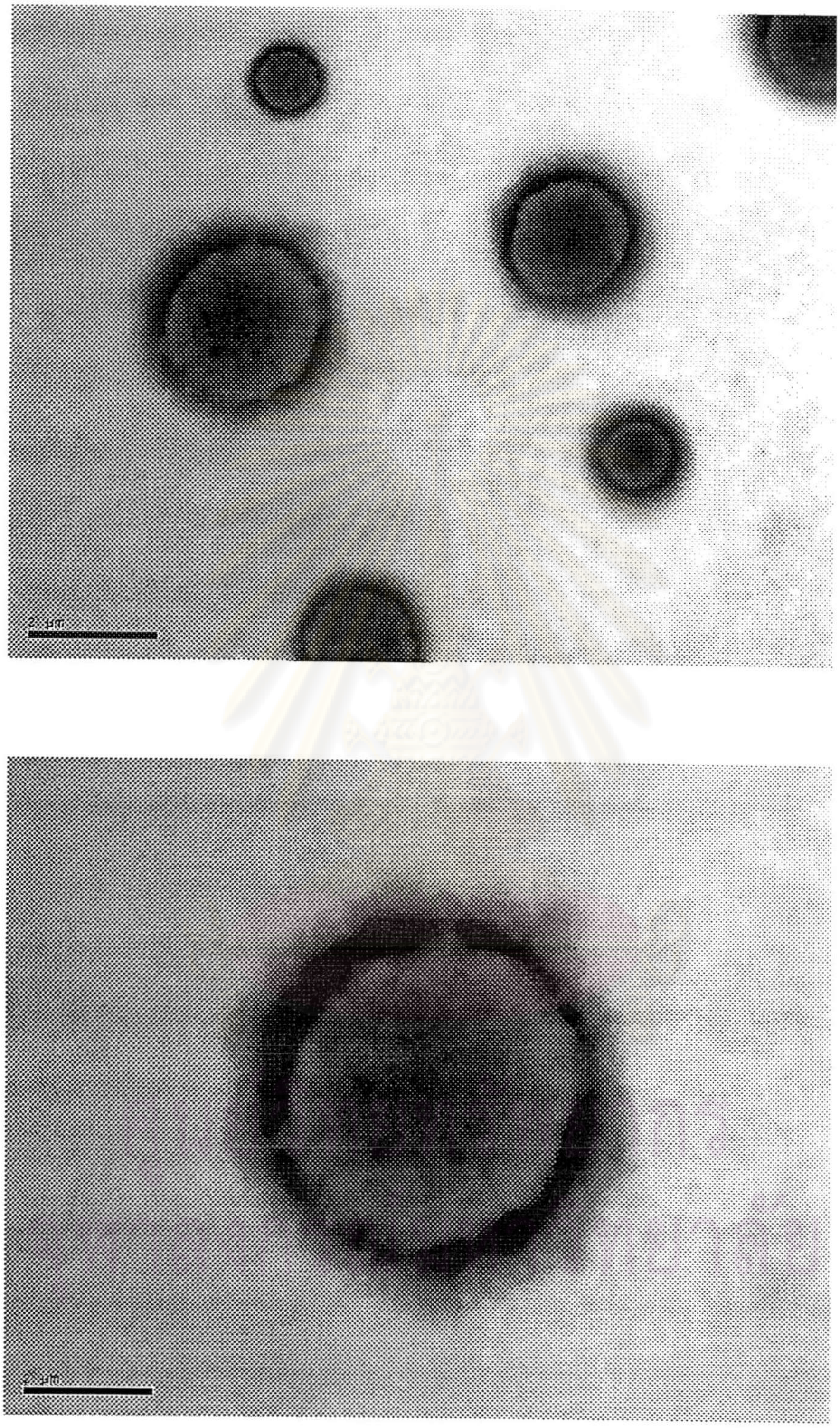

Figure 4-28 Transmission electron micrographs of NR-*g*-poly(DMAEMA) latex particles negatively stained with 1% phosphotungstic acid (PTA); bar is for 2 μm.

indicating that the poly(DMAEMA) is distributed continuously on the surface of NR particle as shown in Figure 4-27.

On the other hand, Figure 4-28 show transmission electron micrographs of the grafted natural rubber latex particle prepared from the same latex as that shown in Figure 4-27. Phosphotungstic acid (PTA) is used as a negative stain. The darker areas revealed the surface of natural rubber particle and the lighter regions show irregular outer layer of poly(DMAEMA) shell. Peng et al. (126) found similar results when they used phosphotungstic acid as negative stain for studying the morphology of polybutadiene/PMMA composite latex particles. In addition, the number-average particle size was determined by measuring a lot of particles in TEM pictures. It was found that the latex particle size increases continuously with the MMA content.

These phenomena may probably be due to phase separation, that is, the rubber polymer is immiscible with the second grafting polymer, poly(DMAEMA). The solubility poly(DMAEMA) is highly hydrophilic, while that for NR is hydrophobic. Furthermore, it has been demonstrated that grafting of the second-stage polymer onto the core particle produces heterogeneous structures of core-shell morphology, which could be formed by phase separation of the immiscible polymers during polymerization.

4.3.9 Thermal Analysis by DSC

The thermal properties of natural rubber latex were measured using differential scanning calorimetry (DSC). Figure 4-29 shows the differential heat capacity as a function of temperature for natural rubber latex. A glass transition temperature (T_g) of −65.1°C was obtained for natural rubber latex in the current research, which is consistent with that reported in the literature (127). Other reported T_g values for natural rubber are −47°C (128) and −63°C (129). These differences could be due to the technique and sample preparation used in the measurements.

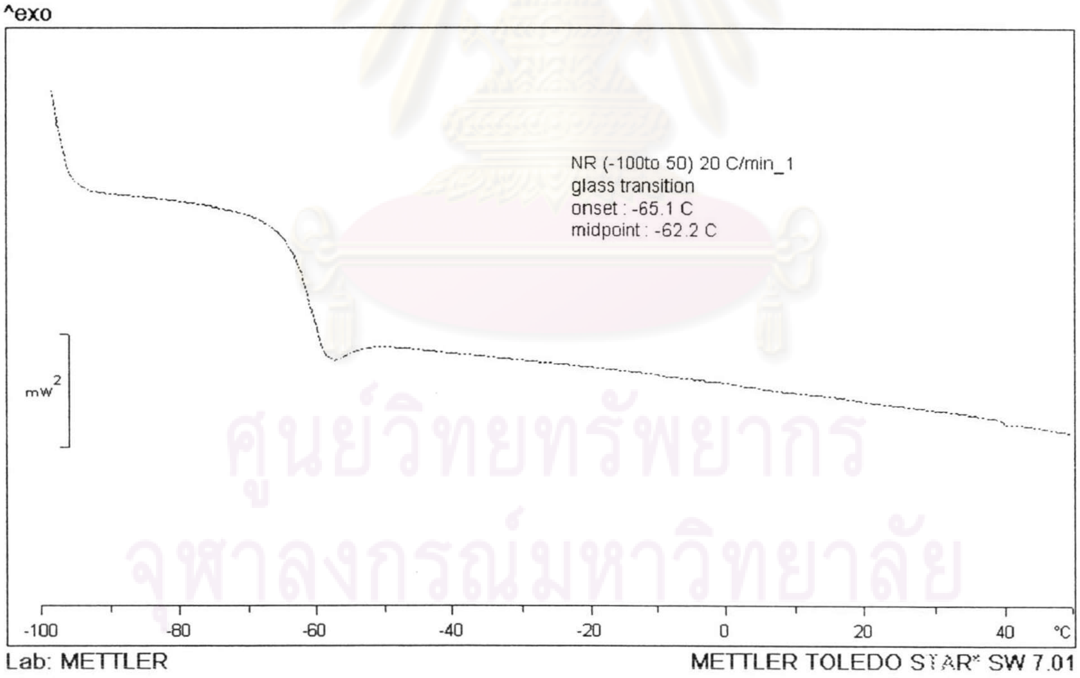

Figure 4-29 DSC thermogram of NR. Scan rate: 20°C min^{-1}.

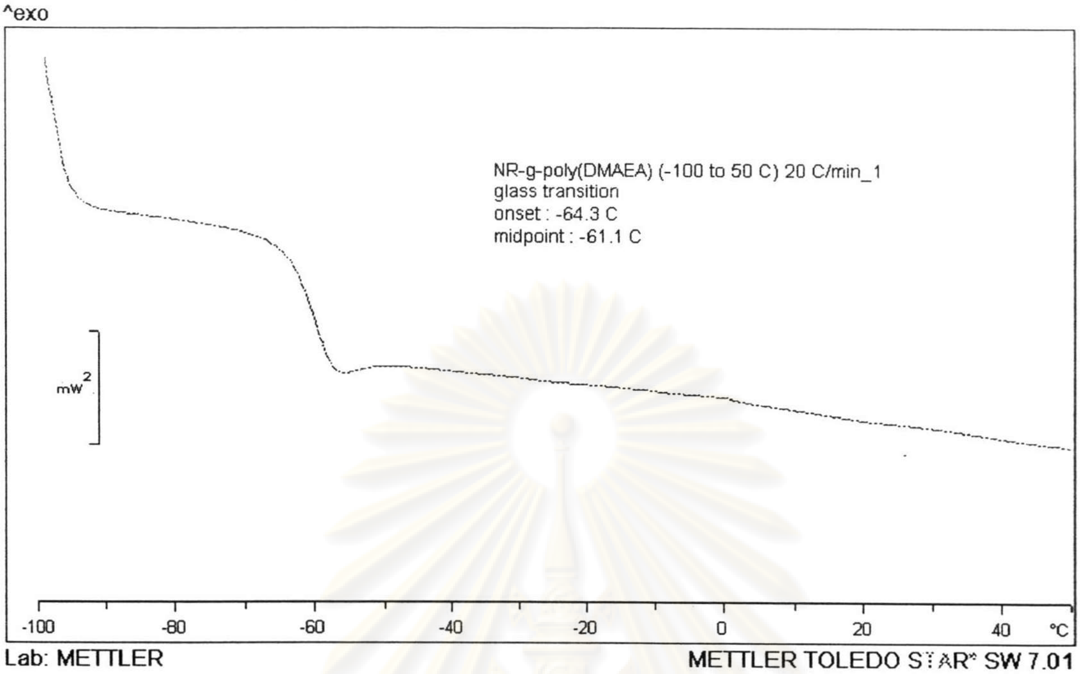

Figure 4-30 DSC thermogram of NR-*g*-poly(DMAEA). Scan rate: 20°C min^{-1}.

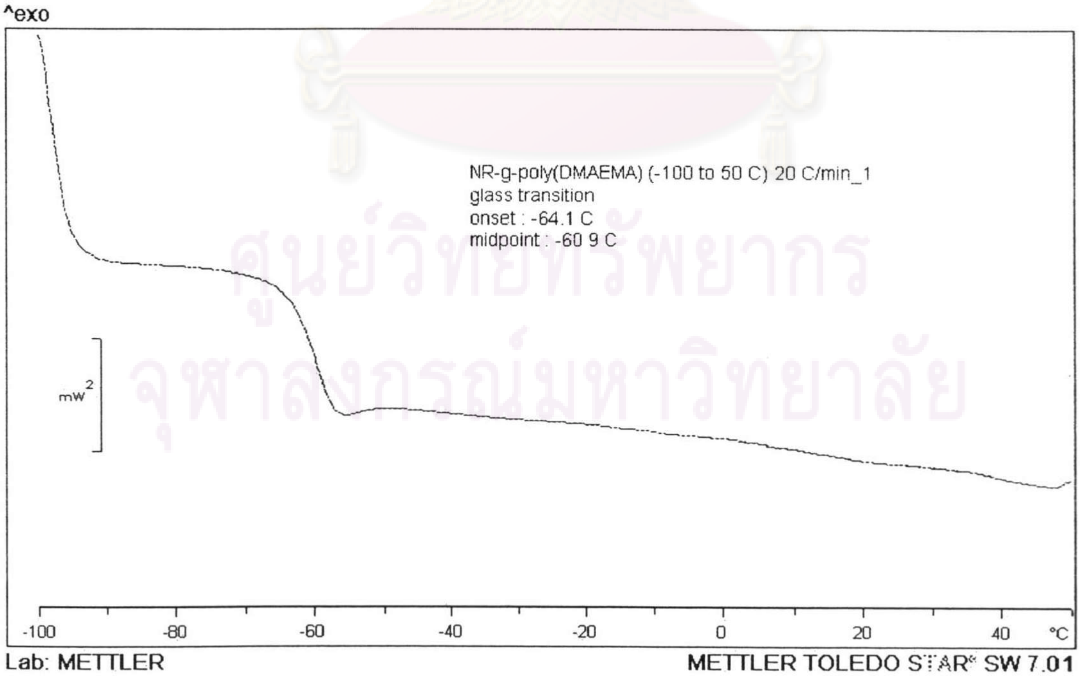

Figure 4-31 DSC thermogram of NR-*g*-poly(DMAEMA). Scan rate: 20°C min^{-1}.

The DSC thermograms of all these latexes revealed only a single T_g as shown in Figures 4-29–4-31. The T_g values of –64.3°C (Figure 4-30) and –64.1°C (Figure 4-31) were obtained for NR-*g*-poly(DMAEA) and NR-*g*-poly(DMAEMA), respectively. In the literature, the T_gs of pure poly(DMAEA) and poly(DMAEMA) measured using DSC are given as –39°C (130) and 19°C (108). There is a slight shift in the glass transition temperature of the natural rubber in both graft copolymers. The T_g is affected by size of the side groups and the mobility of the chains. Any factor disturbing the closest packing of the main chain will lower the T_g; any factor stiffening or increasing the interaction between chains will increase the T_g. This behavior was not observed in the DSC results. The majority of these copolymers has few grafted chains, which are insufficient to affect the free volume of the backbone. The T_g of the backbone could initially be the same for the natural rubber. The insensitive detection of the T_g of the second polymers could be due to the presence of their low amount.

4.3.10 Film Formation

Natural rubber can form a film readily at room temperature due to its rubbery nature. Visual inspection with naked eyes of the film showed no cracks on the surface. In the case of NR-*g*-poly(DMAEA) and NR-*g*-poly(DMAEMA), no cracks on the film were also observed. This is probably due to the homogeneity of NR with both poly(DMAEA) and poly(DMAEMA), and the relatively low T_g's of these artificial polymers. The T_g values for of the NR and homopolymers and grafted copolymers were revealed in Table 4-13.

Table 4-13 T_g data for NR and grafted copolymers

Sample	T_g (°C)
NR	−65.1
NR in the presence of initiator	−63.7
Poly(DMAEA)	−39 (130)
Poly(DMAEMA)	19 (108)
NR-*g*-poly(DMAEA)	−64.3
NR-*g*-poly(DMAEMA)	−64.1

4.3.11 Tensile Properties

The tensile properties of the unmodified and modified NR latexes were determined following ASTM D412. Because these films are not vulcanized the tensile strengths reported in Table 4-14 are green strengths.

From Table 4-14 the tensile strength, stress, and modulus of crosslinked NR film (c-NR) is higher than that of unmodified NR film (NR) and it also increased with increasing the initial DMAEMA monomer concentration. However, elongation did not change significantly.

Table 4-14 Tensile properties of unmodified NR and NR-*g*-poly(DMAEMA) latexes

Run	Tensile Strength (MPa)	Ultimate Elongation (%)	Tensile Stress (MPa)	Modulus at 300% (MPa)
NR	2.32	890	0.49	0.16
c-NR	3.72	980	0.50	0.17
M01	5.82	930	0.63	0.21
M02	6.30	1050	0.67	0.22
M03	6.54	850	1.02	0.34
M04	6.82	1010	1.16	0.39

NR and c-NR are the unmodified NR and crosslinked NR in the presence of initiator, respectively.

The tensile strengths and modulus of the unvulcanized NR from the NR-*g*-poly (DMAEMA) latexes increased substantially above these of the control NR film as the initial monomer concentrations increased.